"APCTP 2016 Workshop on Frontiers of Physics
Dec. 07-09, 2016, Pohang

Equation of State of Compact Star Matter: observable parameters in the era of GW detection

Hyun Kyu Lee
Hanyang University

I. Detection of gravitational waves

II. Binary neutron stars

III. Tidal deformation of star matter

IV. Compact star matter with new scaling law

V. Observational opportunity for measuring tidal deformation

VI. Discussion

I. Detection of gravitational waves from binary black holes

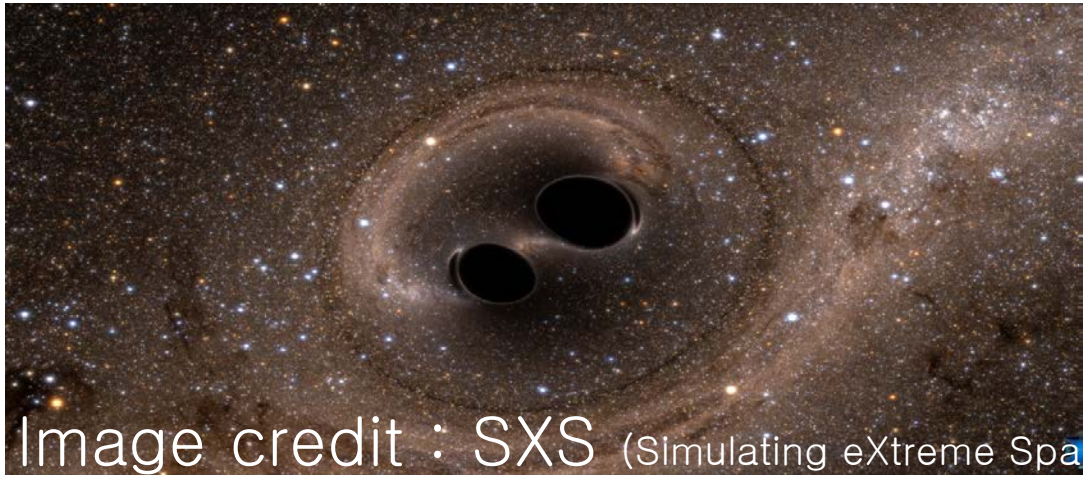

GW150914

GW151226

Selected for a Viewpoint in *Physics*

PRL **116,** 061102 (2016) PHYSICAL REVIEW LETTERS week ending 12 FEBRUARY 2016

Observation of Gravitational Waves from a Binary Black Hole Merger

B. P. Abbott *et al.*[*]
(LIGO Scientific Collaboration and Virgo Collaboration)
(Received 21 January 2016; published 11 February 2016)

On September 14, 2015 at 09:50:45 UTC the two detectors of the Laser Interferometer Gravitational-Wave Observatory simultaneously observed a transient gravitational-wave signal. The signal sweeps upwards in frequency from 35 to 250 Hz with a peak gravitational-wave strain of 1.0×10^{-21}. It matches the waveform predicted by general relativity for the inspiral and merger of a pair of black holes and the ringdown of the resulting single black hole. The signal was observed with a matched-filter signal-to-noise ratio of 24 and a false alarm rate estimated to be less than 1 event per 203 000 years, equivalent to a significance greater than 5.1σ. The source lies at a luminosity distance of 410^{+160}_{-180} Mpc corresponding to a redshift $z = 0.09^{+0.03}_{-0.04}$. In the source frame, the initial black hole masses are $36^{+5}_{-4}M_\odot$ and $29^{+4}_{-4}M_\odot$, and the final black hole mass is $62^{+4}_{-4}M_\odot$, with $3.0^{+0.5}_{-0.5}M_\odot c^2$ radiated in gravitational waves. All uncertainties define 90% credible intervals. These observations demonstrate the existence of binary stellar-mass black hole systems. This is the first direct detection of gravitational waves and the first observation of a binary black hole merger.

DOI: 10.1103/PhysRevLett.116.061102

Primary black hole mass	$36^{+5}_{-4}M_\odot$
Secondary black hole mass	$29^{+4}_{-4}M_\odot$
Final black hole mass	$62^{+4}_{-4}M_\odot$
Final black hole spin	$0.67^{+0.05}_{-0.07}$
Luminosity distance	410^{+160}_{-180} Mpc
Source redshift z	$0.09^{+0.03}_{-0.04}$

PRL **116,** 241103 (2016) PHYSICAL REVIEW LETTERS week ending 17 JUNE 2016

GW151226: Observation of Gravitational Waves from a 22-Solar-Mass Binary Black Hole Coalescence

B. P. Abbott *et al.*[*]
(LIGO Scientific Collaboration and Virgo Collaboration)
(Received 31 May 2016; published 15 June 2016)

We report the observation of a gravitational-wave signal produced by the coalescence of two stellar-mass black holes. The signal, GW151226, was observed by the twin detectors of the Laser Interferometer Gravitational-Wave Observatory (LIGO) on December 26, 2015 at 03:38:53 UTC. The signal was initially identified within 70 s by an online matched-filter search targeting binary coalescences. Subsequent off-line analyses recovered GW151226 with a network signal-to-noise ratio of 13 and a significance greater than 5σ. The signal persisted in the LIGO frequency band for approximately 1 s, increasing in frequency and amplitude over about 55 cycles from 35 to 450 Hz, and reached a peak gravitational strain of $3.4^{+0.7}_{-0.9} \times 10^{-22}$. The inferred source-frame initial black hole masses are $14.2^{+8.3}_{-3.7}M_\odot$ and $7.5^{+2.3}_{-2.3}M_\odot$, and the final black hole mass is $20.8^{+6.1}_{-1.7}M_\odot$. We find that at least one of the component black holes has spin greater than 0.2. This source is located at a luminosity distance of 440^{+180}_{-190} Mpc corresponding to a redshift of $0.09^{+0.03}_{-0.04}$. All uncertainties define a 90% credible interval. This second gravitational-wave observation provides improved constraints on stellar populations and on deviations from general relativity.

DOI: 10.1103/PhysRevLett.116.241103

LSC VIRGO 한국 중력파 연구 협력단
Open Collaboration for the Gravitational Wave Detection and its Application

GW150914

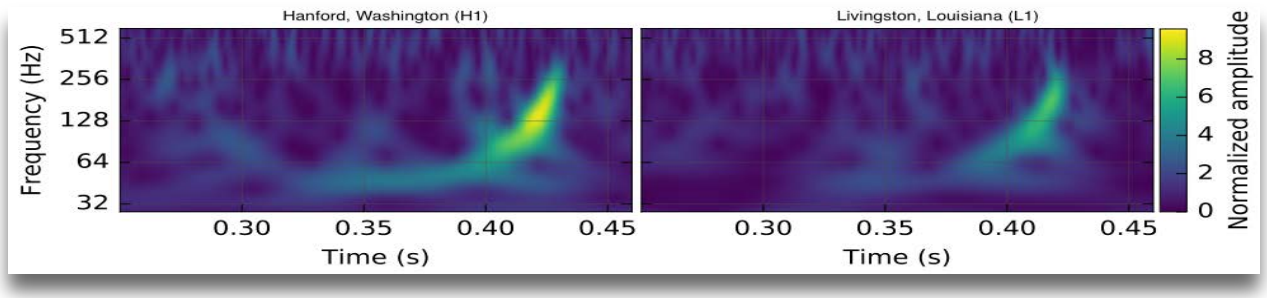
Hanford, Washington (H1)
Livingston, Louisiana (L1)
Frequency (Hz)
512
256
128
64
32
0.30
0.35
0.40
0.45
Time (s)
Normalized amplitude
8
6
4
2
0

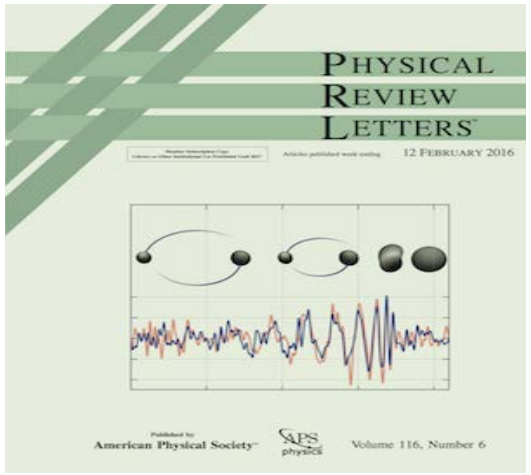
PHYSICAL
REVIEW
LETTERS
12 FEBRUARY 2016
American Physical Society
Volume 116, Number 6

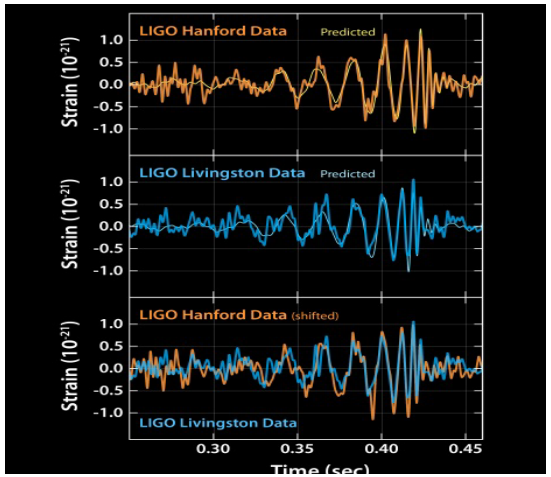
LIGO Hanford Data
Predicted
LIGO Livingston Data
Predicted
LIGO Hanford Data (shifted)
LIGO Livingston Data
Strain (10^{-21})
1.0
0.5
0.0
-0.5
-1.0
0.30
0.35
0.40
0.45
Time (sec)

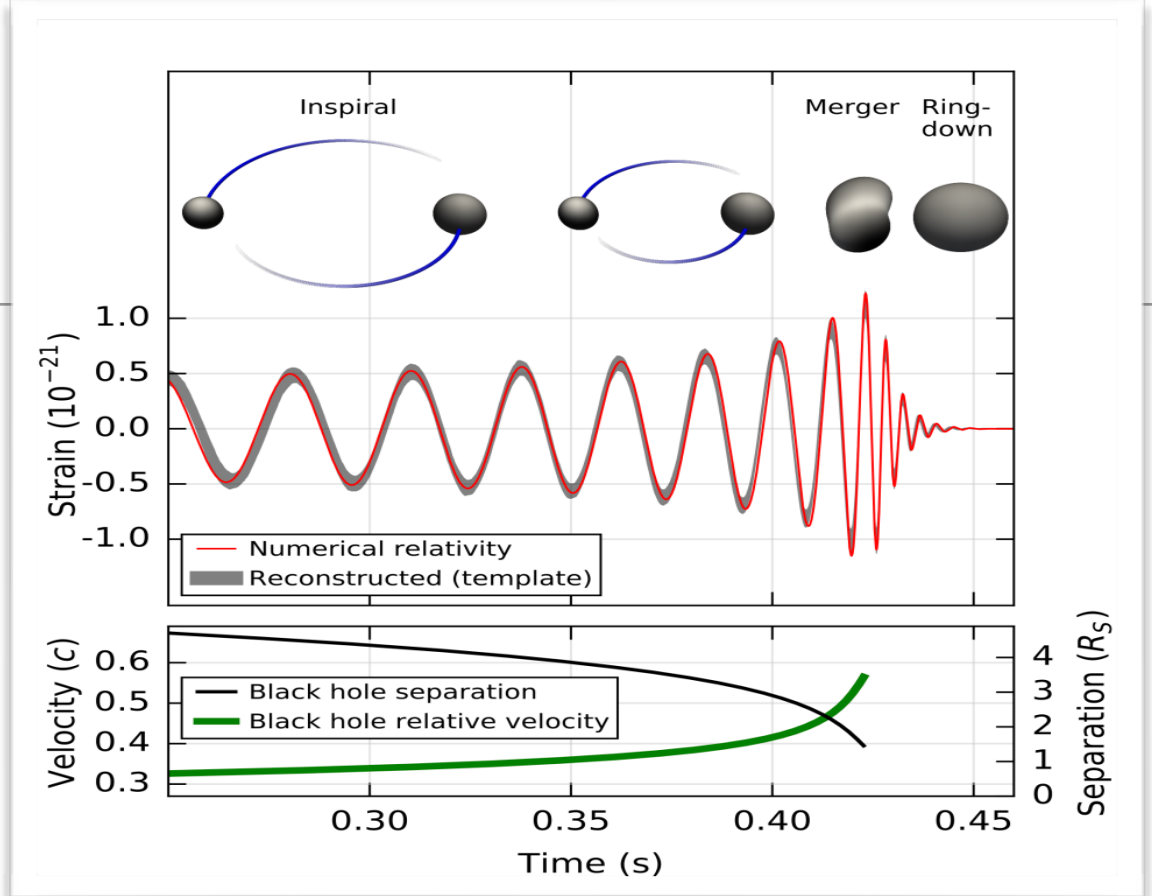
Inspiral
Merger
Ring-down
Strain (10^{-21})
1.0
0.5
0.0
-0.5
-1.0
Numerical relativity
Reconstructed (template)
Velocity (c)
0.6
0.5
0.4
0.3
Black hole separation
Black hole relative velocity
Separation (R_S)
4
3
2
1
0
0.30
0.35
0.40
0.45
Time (s)

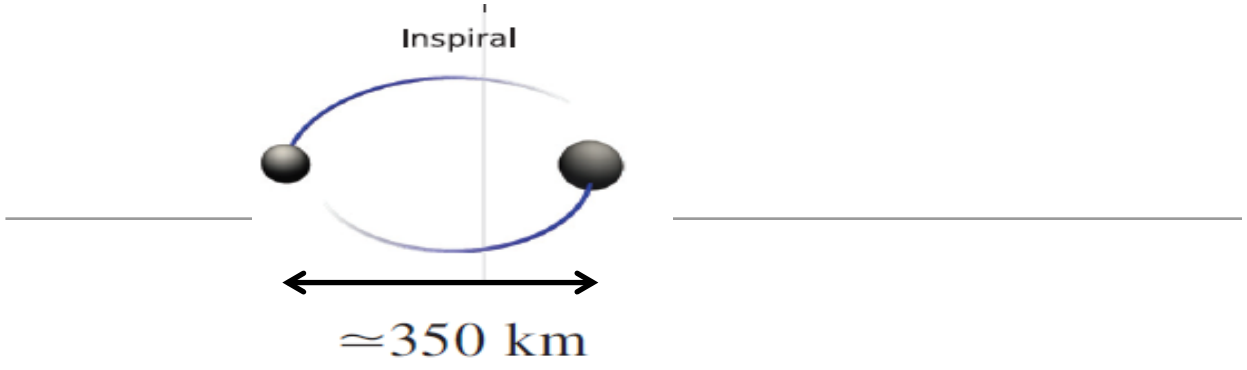

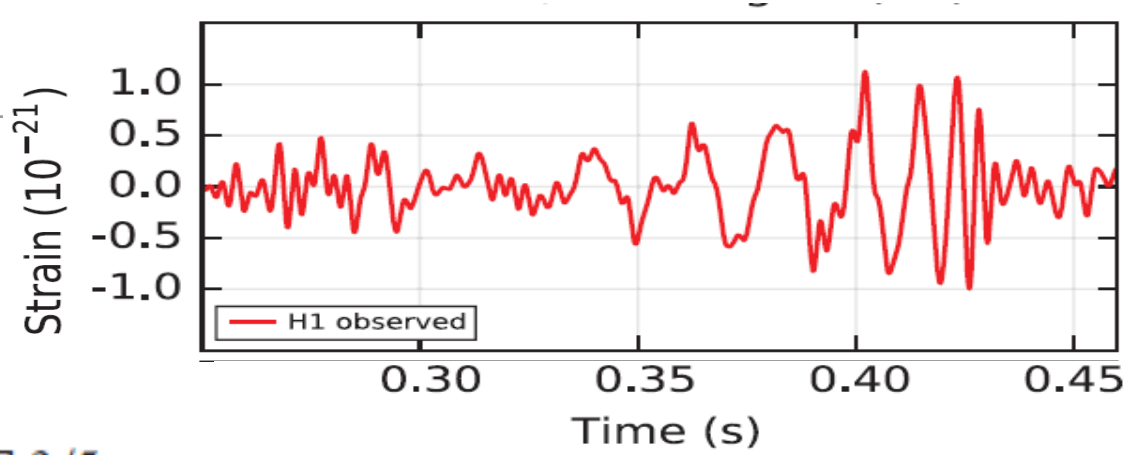

$$\mathcal{M} = \frac{(m_1 m_2)^{3/5}}{(m_1 + m_2)^{1/5}} = \frac{c^3}{G}\left[\frac{5}{96}\pi^{-8/3} f^{-11/3} \dot{f}\right]^{3/5}$$

0.2 s 동안 주파수의 변화 35 - 150 Hz

$$\mathcal{M} \simeq 30 M_\odot \qquad M = m_1 + m_2 \text{ is } \gtrsim 70 M_\odot$$

→ Black hole binary

$$36^{+5}_{-4} M_\odot \text{ and } 29^{+4}_{-4} M_\odot$$

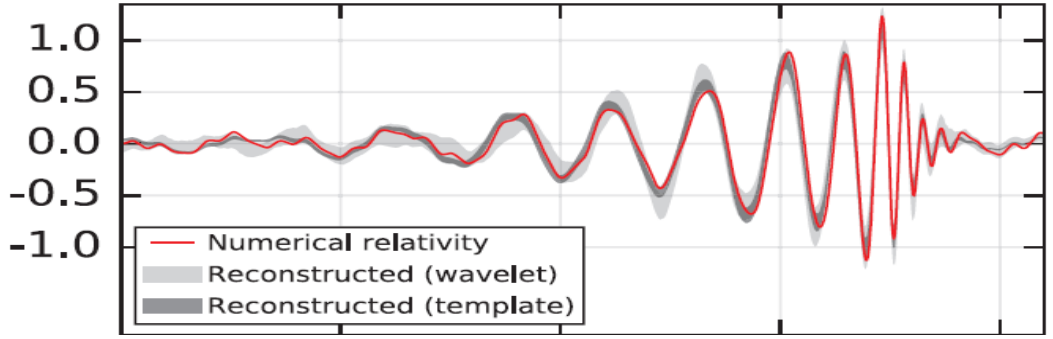

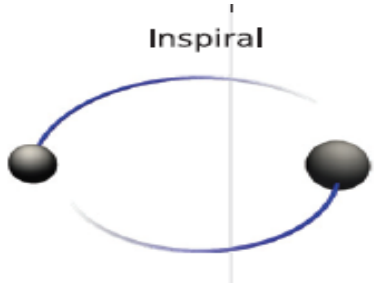

d

h

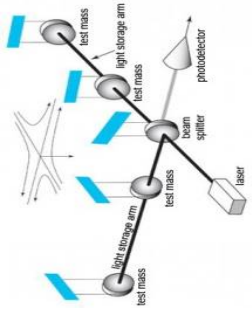

$$d \sim 400\ Mpc$$

$$h = 4\frac{G}{c^4}\frac{\mathcal{M}c^2}{d}\left(\frac{G\mathcal{M}}{c^3}\pi f\right)^{2/3}$$

$$\frac{G}{c^4} = 5 \times 10^{-14}\frac{pc}{M_\odot c^2}$$

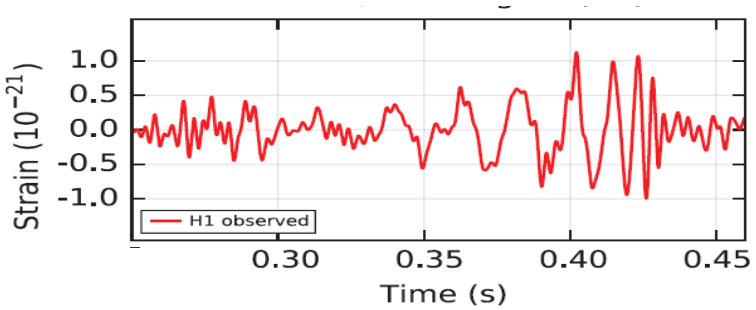

$$h \sim 10^{-21}, \quad \mathcal{M} \sim 30 M_\odot, \quad f \sim 150 Hz$$

$$G = 6.673 \times 10^{-11} m^3 kg^{-1} s^{-2} \qquad \frac{GM_\odot}{c^3} = 0.5 \times 10^{-5} s, \quad \frac{GM_\odot}{c^2} = 1.5 km$$

Arxiv:1606.04856(LIGO/VIRGO)

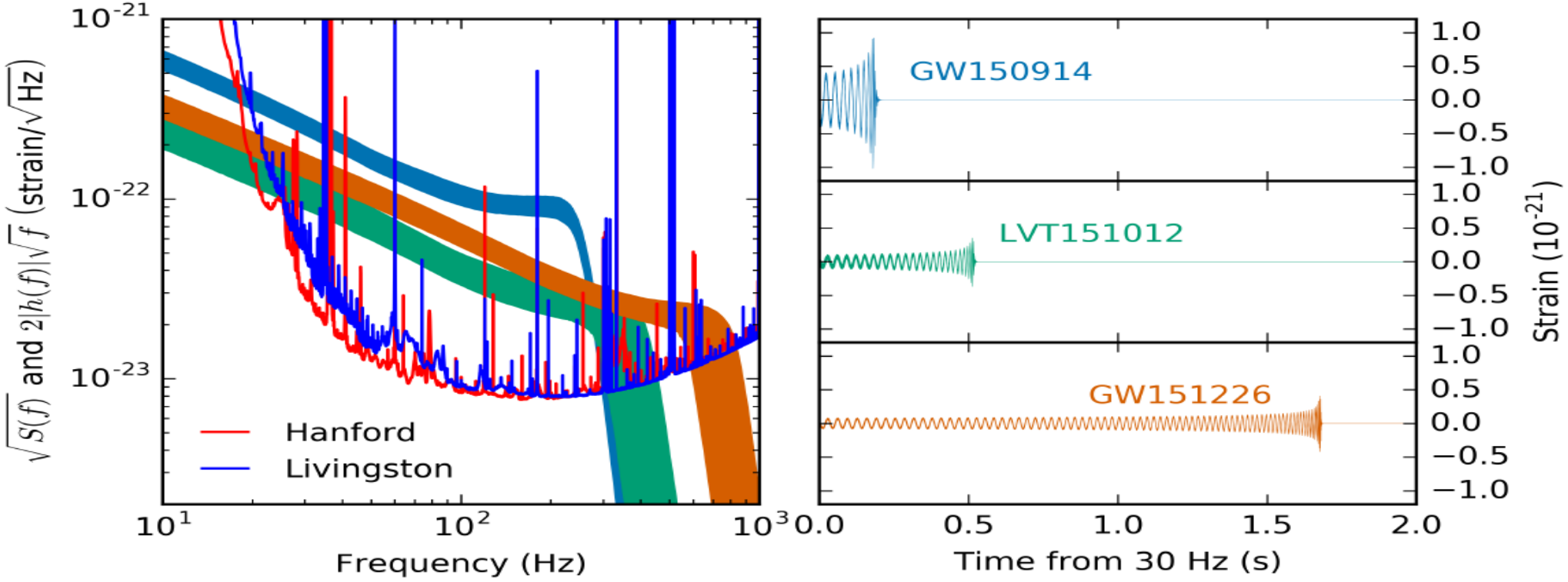

FIG. 1. Left: Amplitude spectral density of the total strain noise of the H1 and L1 detectors, $\sqrt{S(f)}$, in units of strain per $\sqrt{\text{Hz}}$, and the recovered signals of GW150914, GW151226 and LVT151012 plotted so that the relative amplitudes can be related to the SNR of the signa (as described in the text). Right: Time evolution of the waveforms from when they enter the detectors' sensitive band at 30 Hz. All band show the 90% credible regions of the LIGO Hanford signal reconstructions from a coherent Bayesian analysis using a non-precessing spi waveform model [45].

Event	GW150914	GW151226	LVT151012
Signal-to-noise ratio ρ	23.7	13.0	9.7
False alarm rate FAR/yr^{-1}	$< 6.0 \times 10^{-7}$	$< 6.0 \times 10^{-7}$	0.37
p-value	7.5×10^{-8}	7.5×10^{-8}	0.045
Significance	$> 5.3\sigma$	$> 5.3\sigma$	1.7σ
Primary mass $m_1^{\rm source}/{\rm M}_\odot$	$36.2^{+5.2}_{-3.8}$	$14.2^{+8.3}_{-3.7}$	23^{+18}_{-6}
Secondary mass $m_2^{\rm source}/{\rm M}_\odot$	$29.1^{+3.7}_{-4.4}$	$7.5^{+2.3}_{-2.3}$	13^{+4}_{-5}
Chirp mass $\mathscr{M}^{\rm source}/{\rm M}_\odot$	$28.1^{+1.8}_{-1.5}$	$8.9^{+0.3}_{-0.3}$	$15.1^{+1.4}_{-1.1}$
Total mass $M^{\rm source}/{\rm M}_\odot$	$65.3^{+4.1}_{-3.4}$	$21.8^{+5.9}_{-1.7}$	37^{+13}_{-4}
Effective inspiral spin $\chi_{\rm eff}$	$-0.06^{+0.14}_{-0.14}$	$0.21^{+0.20}_{-0.10}$	$0.0^{+0.3}_{-0.2}$
Final mass $M_{\rm f}^{\rm source}/{\rm M}_\odot$	$62.3^{+3.7}_{-3.1}$	$20.8^{+6.1}_{-1.7}$	35^{+14}_{-4}
Final spin $a_{\rm f}$	$0.68^{+0.05}_{-0.06}$	$0.74^{+0.06}_{-0.06}$	$0.66^{+0.09}_{-0.10}$
Radiated energy $E_{\rm rad}/({\rm M}_\odot c^2)$	$3.0^{+0.5}_{-0.4}$	$1.0^{+0.1}_{-0.2}$	$1.5^{+0.3}_{-0.4}$
Peak luminosity $\ell_{\rm peak}/({\rm erg\,s^{-1}})$	$3.6^{+0.5}_{-0.4} \times 10^{56}$	$3.3^{+0.8}_{-1.6} \times 10^{56}$	$3.1^{+0.8}_{-1.8} \times 10^{56}$
Luminosity distance $D_{\rm L}/{\rm Mpc}$	420^{+150}_{-180}	440^{+180}_{-190}	1000^{+500}_{-500}
Source redshift z	$0.09^{+0.03}_{-0.04}$	$0.09^{+0.03}_{-0.04}$	$0.20^{+0.09}_{-0.09}$
Sky localization $\Delta\Omega/{\rm deg}^2$	230	850	1600

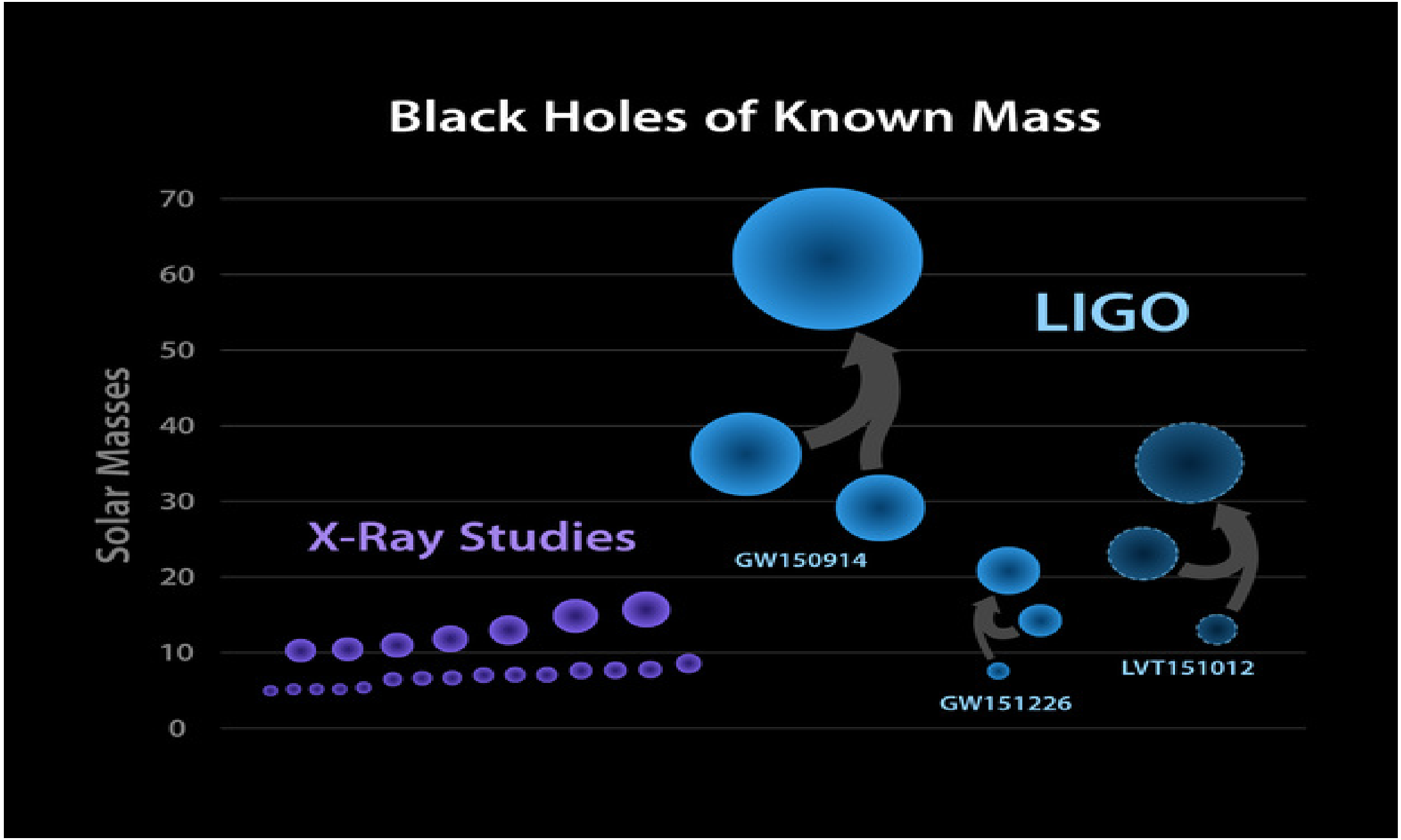
Black Holes of Known Mass
Solar Masses
70
60
50
40
30
20
10
0
LIGO
X-Ray Studies
GW150914
GW151226
LVT151012

II. Binary neutron stars

Observed binary neutron star systems

Biotti and Rezzola arXiv 1607. 03540

Name	$M_{\rm pulsar}$ $[M_\odot]$	$M_{\rm companion}$ $[M_\odot]$	q	$T_{\rm orbit}$ [days]	R [light s]	eccentricity	D [kpc]	$f_{\rm s}$ [Hz]	$B_{\rm surf}$ [G]
J0453+1559	$1.559^{+0.005}_{-0.005}$	$1.174^{+0.004}_{-0.004}$	$0.753^{+0.003}_{-0.003}$	4.072468649(4)	14.4667896(42)	0.11251844(8)	1.83	21.84273295(16)	9.31E+09
J0737-3039	$1.3381^{+0.0007}_{-0.0007}$	$1.2489^{+0.0007}_{-0.0007}$	$0.9333^{+0.0007}_{-0.0007}$	0.102251562(5)	1.415032(1)	0.0877775(9)	1.1	44.05406939(2)	6.39E+09
B1534+12	$1.333^{+0.0004}_{-0.0004}$	$1.3455^{+0.0004}_{-0.0004}$	$0.9907^{+0.0004}_{-0.0004}$	0.420737299(2)	3.7294636(6)	0.27367752(7)	1.05	26.38213278(11)	9.57E+09
J1756-2251	$1.341^{+0.007}_{-0.007}$	$1.23^{+0.007}_{-0.007}$	$0.917^{+0.007}_{-0.007}$	0.319633901(3)	2.756457(9)	0.1805694(2)	0.73	35.13507271(6)	5.44E+09
J1906+0746	$1.291^{+0.011}_{-0.011}$	$1.322^{+0.011}_{-0.011}$	$0.976^{+0.012}_{-0.012}$	0.165993047(11)	1.419962(18)	0.0853028(6)	7.4	6.940918295(2)	–
B1913+16	$1.4398^{+0.0002}_{-0.0002}$	$1.3886^{+0.0002}_{-0.0002}$	$0.9644^{+0.0002}_{-0.0002}$	0.322997449(4)	2.341782(3)	0.6171334(5)	7.13	16.94053779(15)	2.28E+10
B2127+11C	$1.358^{+0.01}_{-0.01}$	$1.354^{+0.01}_{-0.01}$	$1.00^{+0.01}_{-0.01}$	0.335282048(5)	2.51845(6)	0.681395(2)	12.9	32.7554227(11)	1.25E+10
J1518+4904	$1.766^{+0.003}_{-0.991}$	$0.951^{+0.995}_{-0.001}$	$0.5^{+0.5}_{-0.3}$	8.634005096(11)	20.0440029(4)	0.24948451(3)	0.7	24.42897938(3)	9.62E+08
J1811-1736	$1.478^{+0.137}_{-0.71}$	$1.002^{+0.872}_{-0.056}$	$0.7^{+0.6}_{-0.3}$	18.7791691(4)	34.7827(5)	0.828011(9)	5.93	9.598591253(4)	–
J1829+2456	$1.298^{+0.034}_{-0.843}$	$1.273^{+0.872}_{-0.019}$	$1.00^{+0.7}_{-0.6}$	1.176027941(16)	7.238(2)	0.1391412(19)	0.74	24.38440141(3)	–
J1930-1852	$1.199^{+0.059}_{-0.79}$	$1.363^{+0.831}_{-0.034}$	$0.9^{+0.5}_{-0.6}$	45.0600007(5)	86.890277(7)	0.3988634(17)	2.34	5.390249757(3)	–

gravitational radiation: yet too weak to be detected at LIGO

- No observation in O1 run of advanced LIGO.
- Advanced LIGO could have detected
  - binary neutron star with ~1.35 solar mass at ~ 70 Mpc
  - binary black hole neutron star with 5 solar mass black hole at ~ 110Mpc
- Upper limit on merger rates Biotti and Rezzola arXiv 1607. 03540

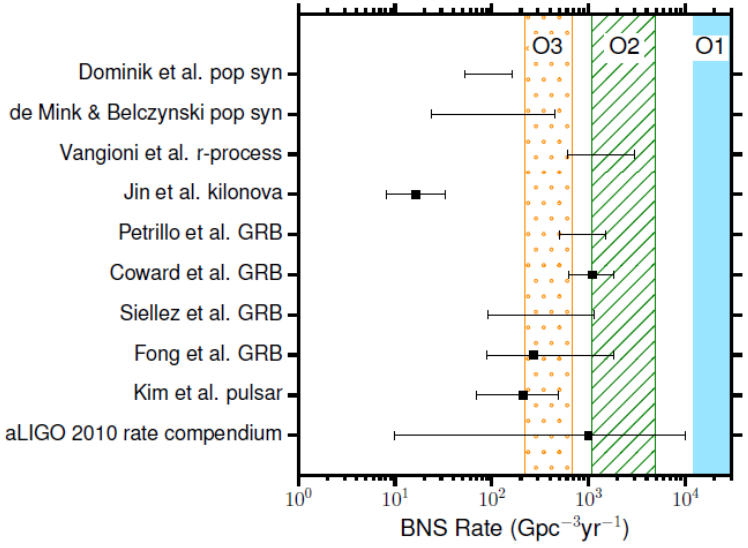

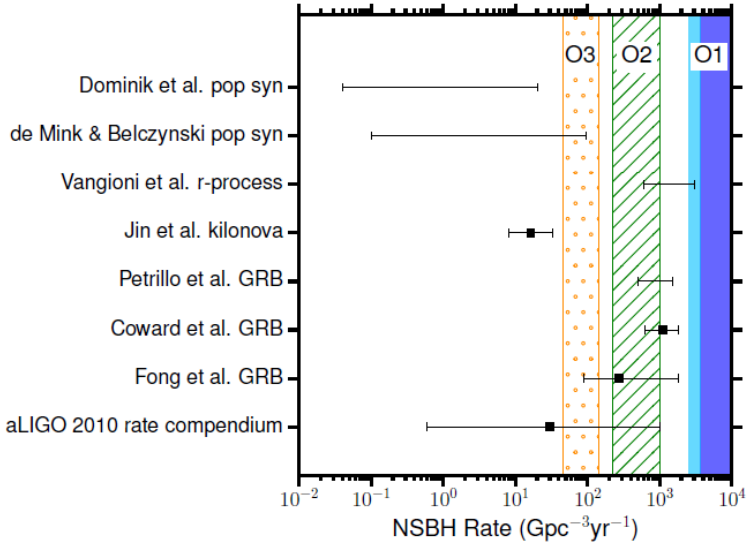

LIGO-Commencement of Observing Run O2 on Wednesday, November 30th, 2016

- # Strain sensitivity curve and estimated merger rates

J. Aasi et al., Living Rev. Rel. 19, 1(2016) arXiv 1304.0670

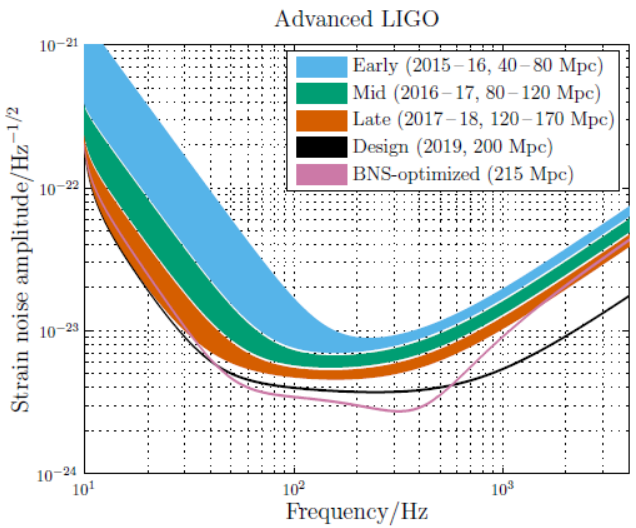

Epoch			2015 – 2016	2016 – 2017	2017 – 2018	2019+	2022+ (India)
Estimated run duration			4 months	6 months	9 months	(per year)	(per year)
Burst range/Mpc		LIGO	40 – 60	60 – 75	75 – 90	105	105
		Virgo	—	20 – 40	40 – 50	40 – 80	80
BNS range/Mpc		LIGO	40 – 80	80 – 120	120 – 170	200	200
		Virgo	—	20 – 60	60 – 85	65 – 115	130
Estimated BNS detections			0.0005 – 4	0.006 – 20	0.04 – 100	0.2 – 200	0.4 – 400
90% CR	% within	5 deg^2	< 1	2	*$> 1 - 2$*	*$> 3 - 8$*	*> 20*
		20 deg^2	< 1	14	*> 10*	*$> 8 - 30$*	*> 50*
	median/deg^2		480	230	—	—	—
searched area	% within	5 deg^2	6	20	—	—	—
		20 deg^2	16	44	—	—	—
	median/deg^2		88	29	—	—	—

GW1612XX

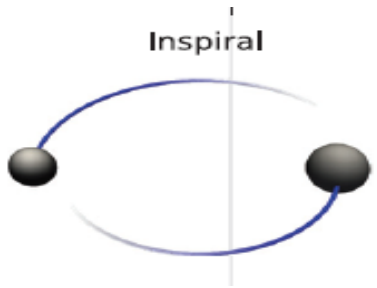

d ⟷ h

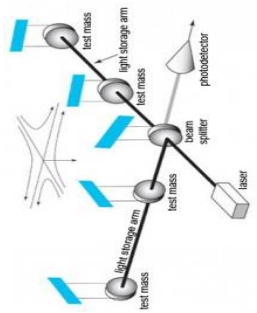

$$\mathcal{M} = \frac{(m_1 m_2)^{3/5}}{(m_1 + m_2)^{1/5}} = \frac{c^3}{G}\left[\frac{5}{96}\pi^{-8/3} f^{-11/3} \dot{f}\right]^{3/5}$$

$$\mathcal{M} \sim 1 m_\odot$$

$$h = 4\frac{G}{c^4}\frac{\mathcal{M}c^2}{d}\left(\frac{G\mathcal{M}}{c^3}\pi f\right)^{2/3}$$

$$\frac{G}{c^4} = 5 \times 10^{-14}\frac{pc}{M_\odot c^2}$$

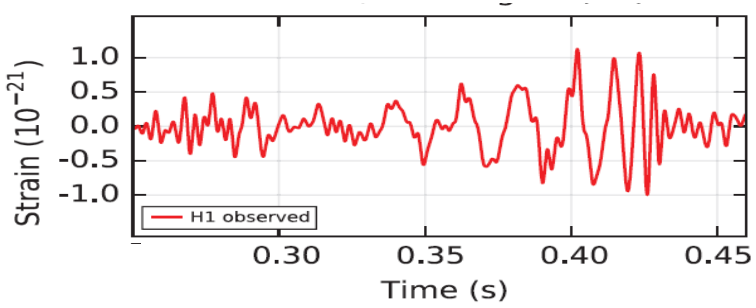

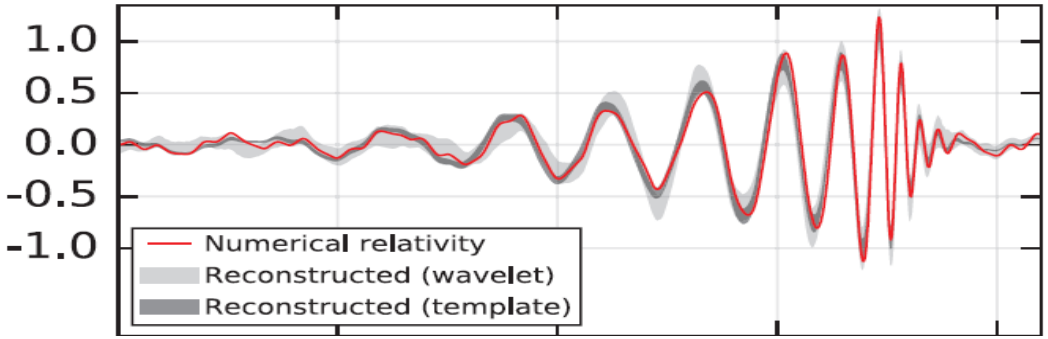

binary neutron stars

Gravitational Wave from Orbiting Binary System

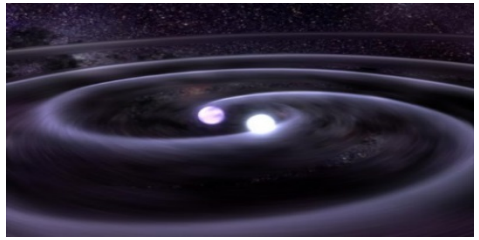

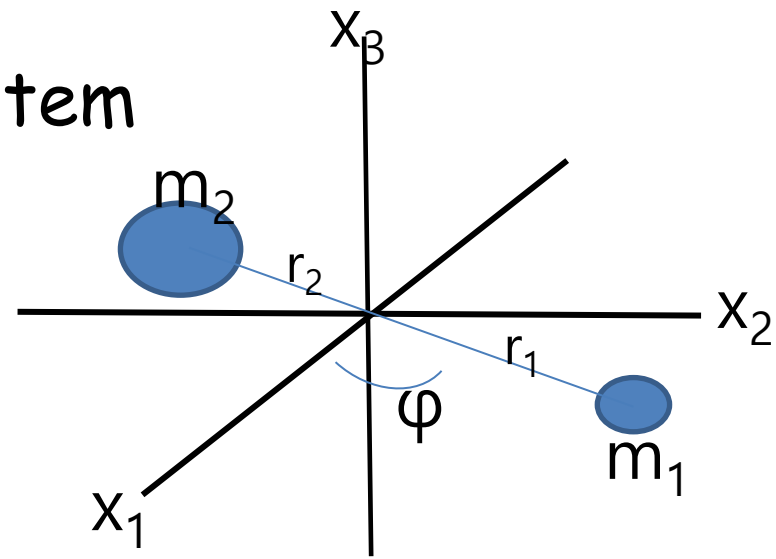

- reduced mass $$\mu = \frac{m_1 m_2}{M}$$
- symmetric mass ratio $$\eta = \frac{\mu}{M}$$
- Keplerian angular velocity

$$\omega = \sqrt{\frac{GM}{a^3}} \qquad a = r_1 + r_2$$

- Gravitational wave

$$h_+ = -\frac{2G\mu}{c^2 r}(1+\cos^2\iota)(\frac{\nu}{c})^2\cos 2\phi$$

$$h_\times = -\frac{2G\mu}{c^2 r}\cos^2\iota(\frac{\nu}{c})^2\sin 2\phi$$

$$\nu = (2\pi G M f)^{1/3}$$

$$\phi = \omega t \qquad f = 2 f_{orbital} = \omega/\pi$$

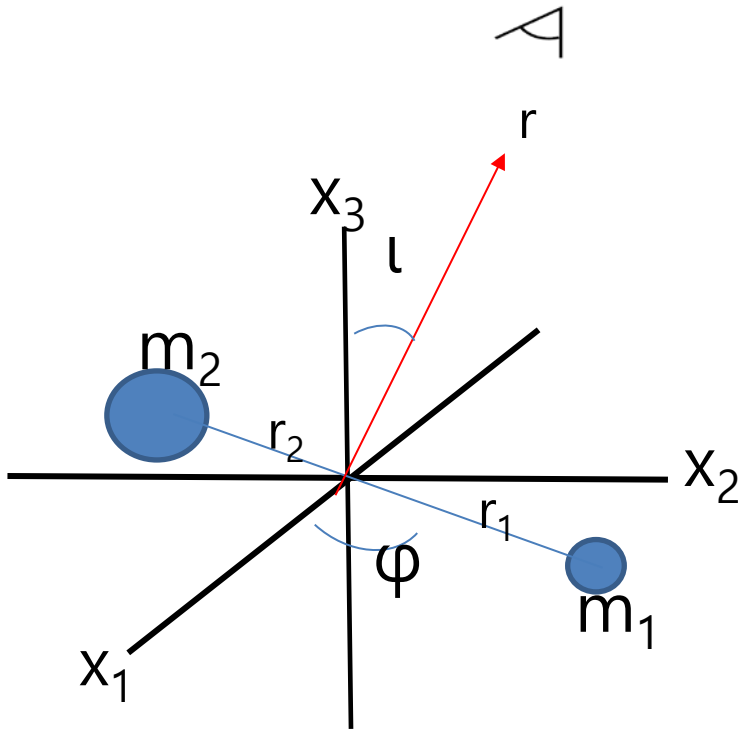

- Ripples in the curvature of space-time

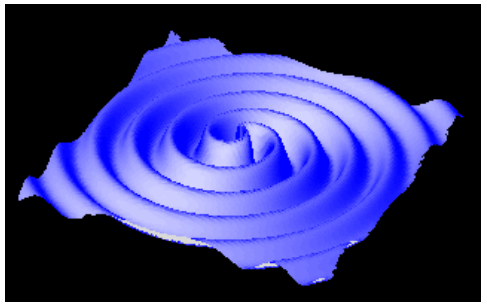

- Mass and radius

Tolman-Oppenheimer-Volkov equations

$$\frac{dp}{dr} = -\frac{G}{c^4}\frac{(mc^2 + 4\pi p r^3)(\varepsilon + p)}{r(r - 2Gm/c^2)}$$

$$\frac{dm}{dr} = 4\pi \frac{\varepsilon}{c^2} r^2$$

Equation of state :

pressure and energy density

Phases of Dense Matter in Neutron Stars

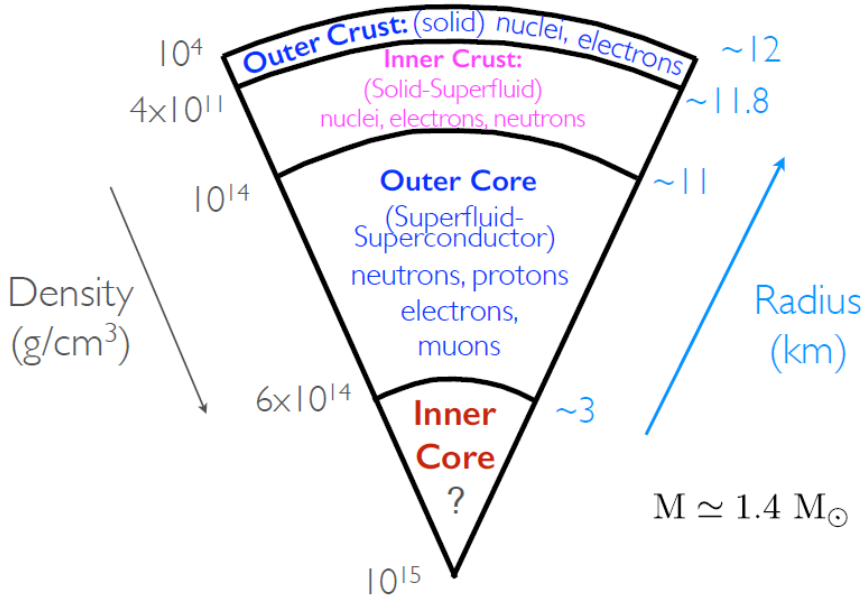

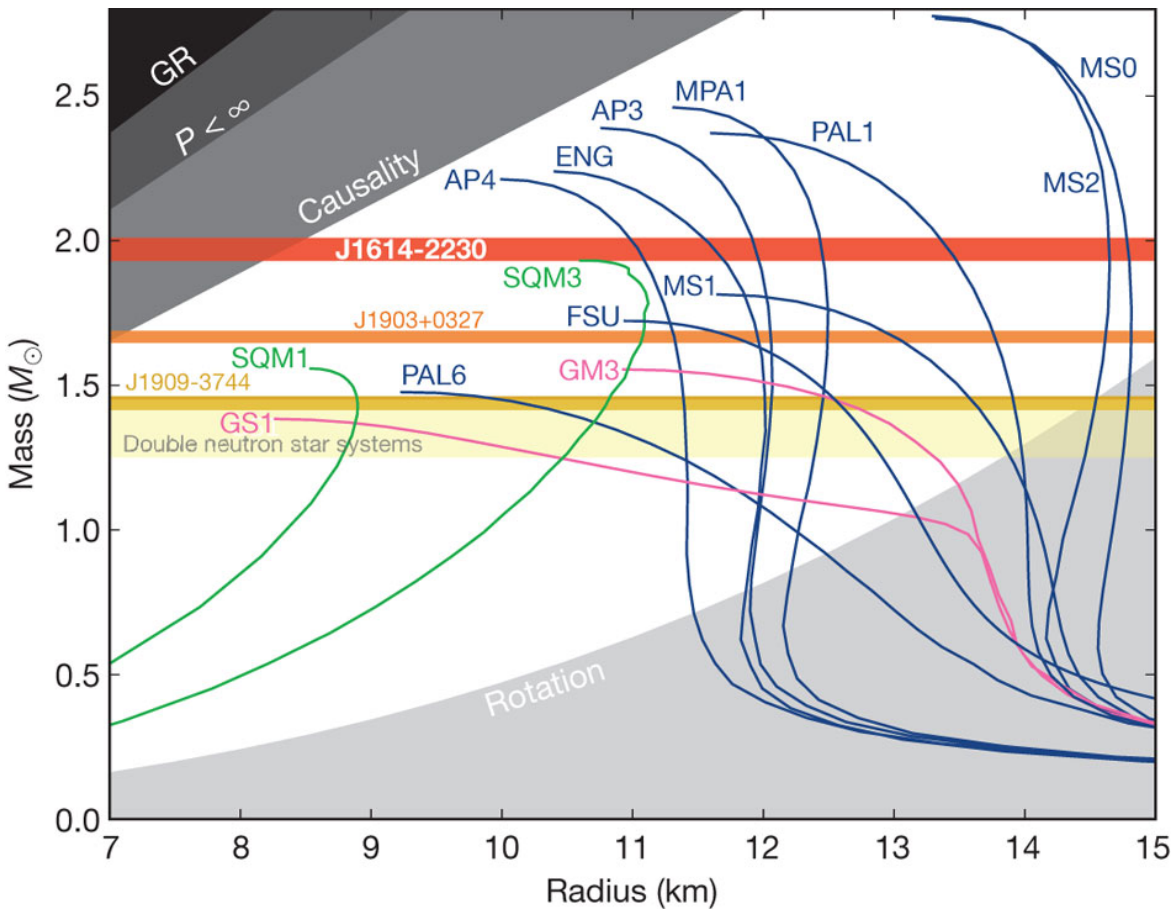

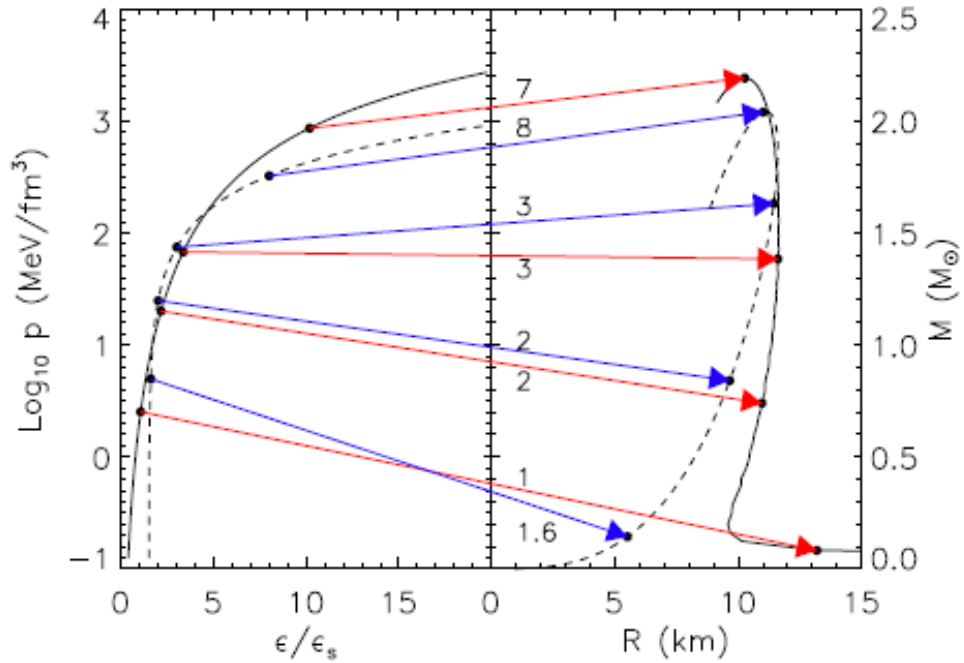

Lattimer, arXiv: 1305.3510

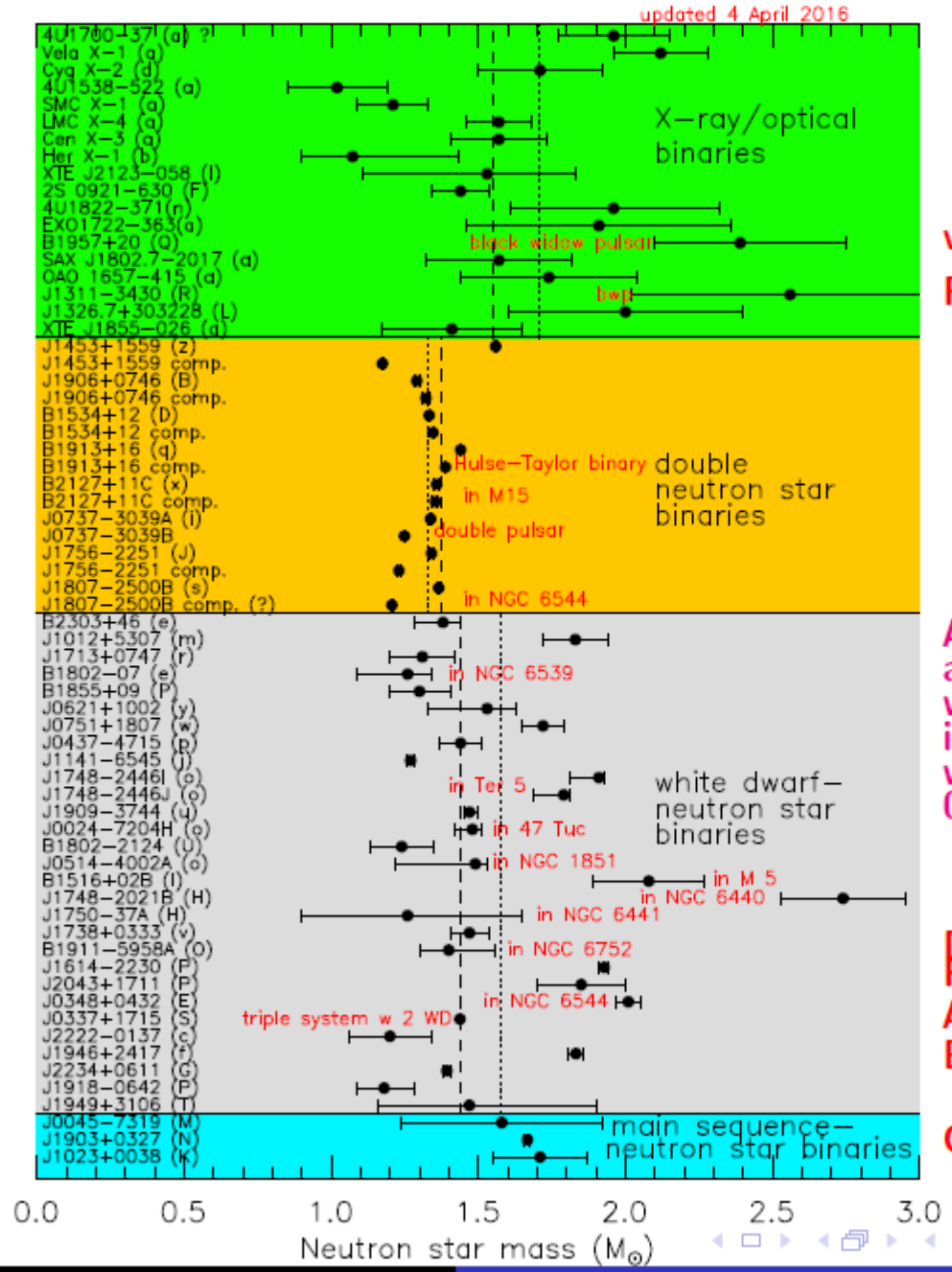

vanKerkwijk 2010

Romani et al. 2012

Although simple average mass of w.d. companions is 0.23 $M_\odot$ larger, weighted average is 0.04 $M_\odot$ smaller

Demorest et al. 2010
Fonseca et al. 2016
Antoniadis et al. 2013
Barr et al. 2016

Champion et al. 2008

III. Tidal deformation of star matter

- Tidal deformation during merger stage

- Departure from point particle approximation :

- Change in gravitational wave form

$$\frac{dE}{dt} = -L_{GW} \Rightarrow \nu(t)(f(t))$$

$$\frac{d\phi}{dt} = \pi f \Rightarrow \phi(t)$$

A. Tidal deformation

- Metric around deformed body due to external quadrupole field

$$\mathcal{E}_{ij}$$

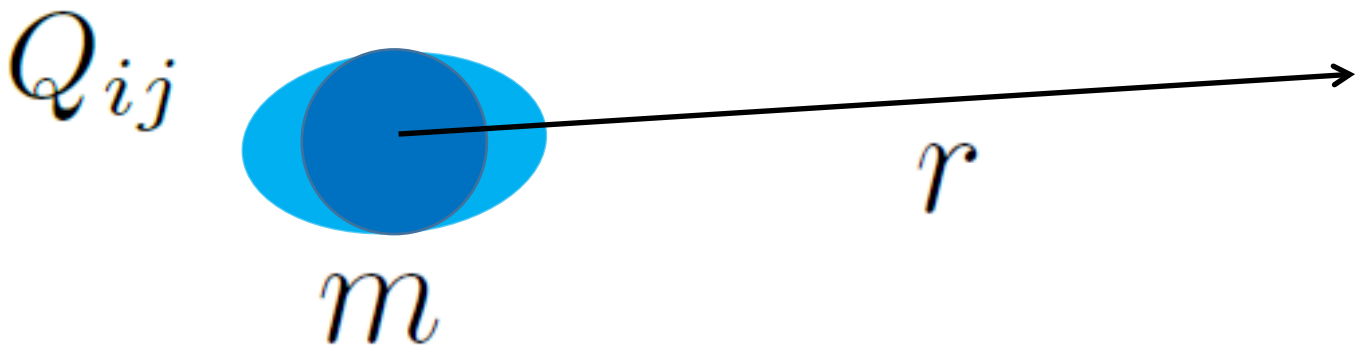

$$\frac{1+g_{00}}{2} = \frac{m}{r} + \frac{3}{2}\frac{Q_{ij}}{r^3}n^i n^j - \frac{1}{2}\mathcal{E}_{ij}r^2 n^i n^j + \cdots$$

- Applied quadrupole tidal field $\mathcal{E}_{ij}$ (symmetric and traceless)
- Induced quadratic moment Q_{ij}
- Tidal deformability λ

$$Q_{ij} = -\lambda \mathcal{E}_{ij}$$

Equation of state(EoS) → mass, radius,
tidal deformability, ...

B. Basic Equations

A. Tolman-Oppenheimer-Volkov(TOV) Equation

- metric for a spherically symmetric(static, non-rotating) configuration

$$ds^2 = -e^{\Phi(r)}dt^2 + e^{\Lambda(r)}dr^2 + r^2 d\theta^2 + r^2 \sin^2\theta d\phi^2$$

$$e^{\Lambda(r)} = (1 - \frac{2m}{r})^{-1}$$

- perfect-fluid stellar matter

$$T_{\mu\nu} = (\epsilon + p)u_\mu u_\nu + p g_{\mu\nu}$$

- Tolman-Oppenheimer-Volkov(TOV) Equation

$$\frac{dm}{dr} = 4\pi r^2 \epsilon$$

$$\frac{dp}{dr} = -(\epsilon + p)\frac{m + 4\pi r^3 p}{r(r - 2m)}$$

$$\frac{d\Phi}{dr} = -\frac{1}{\epsilon + p}\frac{dp}{dr}$$

B. Einstein field equation for perturbation

- Linearized perturbation

$$g_{\mu\nu} = g^{(0)}_{\mu\nu} + h_{\mu\nu}$$

TOV Eqs.

$$h_{\mu\nu} = diag\big[-e^{2\Phi(r)} H(r) Y_{20}(\theta,\phi), \\ -e^{2\Lambda(r)} H(r) Y_{20}(\theta,\phi), \\ -r^2 K(r) Y_{20}(\theta,\phi), \\ -r^2 \sin^2\theta K(r) Y_{20}(\theta,\phi)\big]$$

$$\delta T^0_0 = -\delta\epsilon(r) Y_{20}, \quad \delta T^i_i = \delta p(r) Y_{20}$$

$$\delta G_{\mu\nu} = 8\pi \delta T_{\mu\nu}$$

$$H'' + \left(\frac{2}{r} + \Phi' - \Lambda'\right) H' \\ + \left\{ 2(\Phi'' - \Phi'^2) - \frac{6}{r^2} e^{2\Lambda} + \frac{3}{r}\Lambda' \\ + \frac{7}{r}\Phi' - 2\Phi'\Lambda' + \frac{f}{r}(\Phi' + \Lambda') \right\} H = 0$$

$$f(r) = \frac{d\epsilon}{dp}$$

C. Deformability

- Continuity of $H(r)$ and $H'(r)$ at the boundary, r=R

$\Phi(r) \quad m(r)$ ⟵ Equation of State

- Asymptotic form

$$\frac{1+g_{00}}{2} = \frac{m}{r} + \frac{3}{2}\frac{Q_{ij}}{r^3}n^i n^j - \frac{1}{2}\mathcal{E}_{ij}r^2 n^i n^j + \cdots$$

$$\boxed{-\frac{1+g_{00}}{2} \to -\left[\frac{M}{r} - \frac{1}{2}H^{asympt}(r)Y_{20}\right]}$$

- Asymptotic solution

$$H^{asympt} = \frac{8}{5}\left(\frac{M}{r}\right)^3 c_1 + \left(\frac{r}{M}\right)^2 c_2 \cdots$$

- Deformability

$$\boxed{\lambda = \frac{8}{15} M^5 \frac{c_1}{c_2}}$$

$$\lambda = \frac{16}{15} R^5 C^5 (1-2C)^2 [2 + 2C(y-1) - y]$$
$$\times \Big\{ 2C[6 - 3y + 3C(5y-8)] + 4C^3[13 - 11y + C(3y-2) + 2C^2(1+y)]$$
$$+ 3(1-2C)^2[2 - y + 2C(y-1)] \ln(1-2C) \Big\}^{-1}$$

$$y = RH'(R)/H(R) \quad C = M/R$$

- dimensionless tidal deformation parameter

$$\Lambda = G\lambda\left(\frac{c^2}{Gm}\right)^5$$

$$m = (1.35, 1.4, 2.0) m_\odot$$

$$\Lambda = (2.14, 1.78, 0.297) \times 10^2 \left(\frac{\lambda}{10^{36} g cm^2 s}\right)$$

Example 1. Postnikov, Prakash and Lattimer Phys.Rev.D82, 024016(2010)

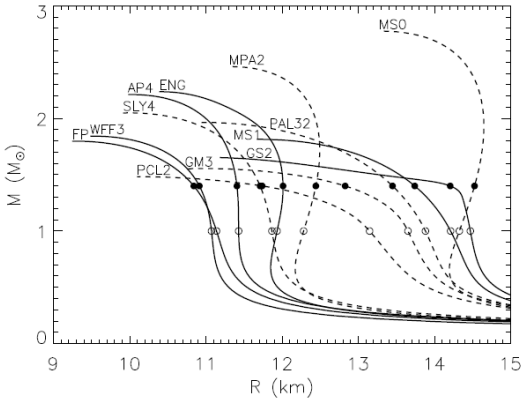

FIG. 6: Mass-radius diagram for the hadronic equation of states used in this paper. Filled (open) circles indicate configurations with $M = 1.4$ $M_\odot$ (1.0 $M_\odot$). The EOS notation follows Lattimer and Prakash [6] and Table I.

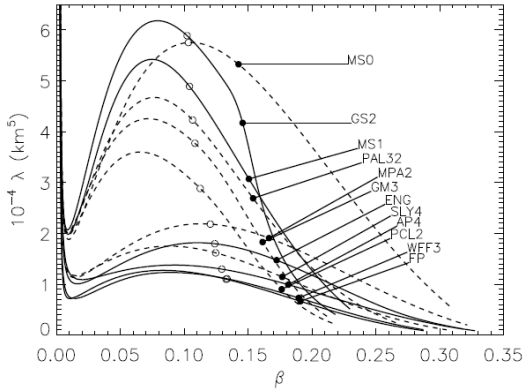

FIG. 9: The quantity $\lambda = (2/3)k_2R^5$ for hadronic equations of state. Filled (open) circles indicate configurations with $M = 1.4$ $M_\odot$ (1.0 $M_\odot$).

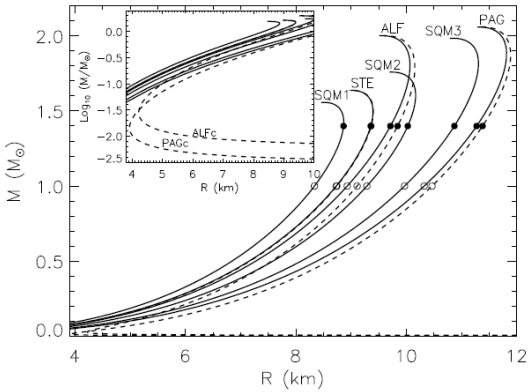

FIG. 12: Mass-radius curves for strange quark matter equations of state. The insert shows results on a logarithmic scale to highlight the effects of a hadronic crust.

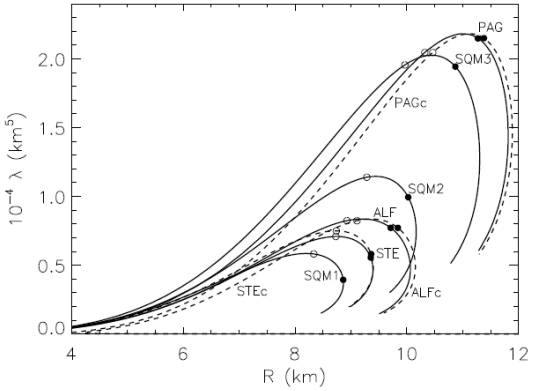

FIG. 14: Quadrupole polarizabilities λ for the strange quark matter stars. Filled (open) circles indicate configurations with $M = 1.4$ $M_\odot$ (1.0 $M_\odot$).

Example 2. Hinderer et al., Phys. Rev. D 81,123016(2010)

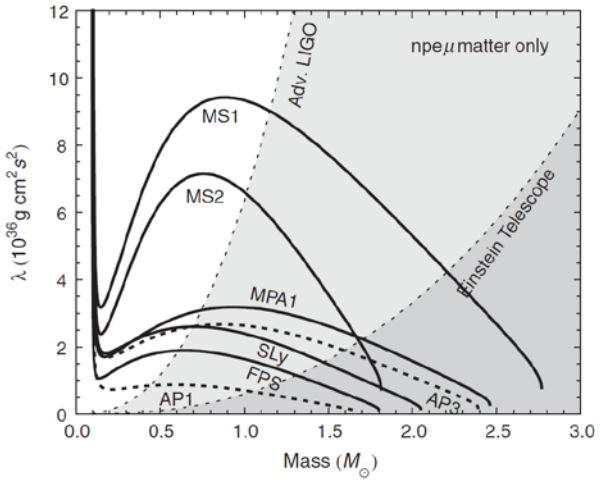

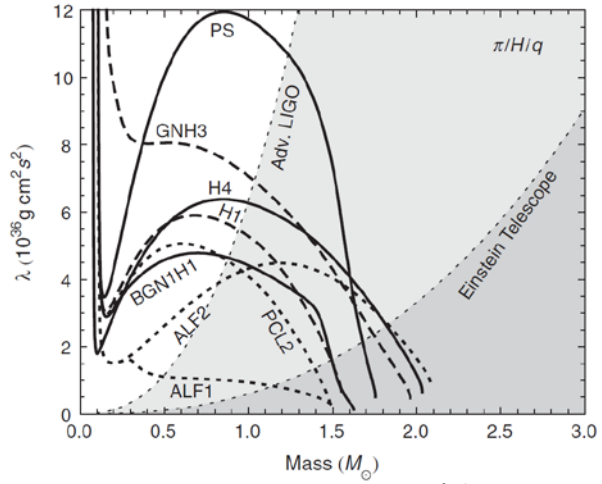

10-450 Hz window

EOS	R (km)	m/R	k_2	$\lambda(10^{36}$ g cm^2 s$^2)$
SLY	11.74	0.176	0.0763	1.70
AP1	9.36	0.221	0.0512	0.368
AP3	12.09	0.171	0.0858	2.22
FPS	10.85	0.191	0.0663	1.00
MPA1	12.47	0.166	0.0924	2.79
MS1	14.92	0.139	0.110	8.15
MS2	13.71	0.151	0.0883	4.28
PS	15.47	0.134	0.104	9.19
BGN1H1	12.90	0.160	0.0868	3.10
GNH3	14.20	0.146	0.0867	5.01
H1	12.86	0.161	0.0738	2.59
H4	13.76	0.150	0.104	5.13
PCL2	11.76	0.176	0.0577	1.30
ALF1	9.90	0.209	0.0541	0.513
ALF2	13.19	0.157	0.107	4.28
SQM1	8.86	0.233	0.098	0.536
SQM2	10.03	0.206	0.136	1.38
SQM3	10.87	0.190	0.166	2.52

$1.4m_\odot$

Example 3. Hotokezaka, Kyutoku, Sekiguchi, Shibata. Rev. D93, 064082(2016)

EOS	$M_{\max}$ ($M_\odot$)	$R_{1.35}$ (km)	Λ	$k_{2,1.35}$	$k_{3,1.35}$	$k_{4,1.35}$	$m_0\Omega_0$	L (km)	Δx (km)
APR4	2.20	11.09	322	0.0908	0.0234	0.00884	0.0156	2572	0.167, 0.209, 0.251
SFHo	2.06	11.91	420	0.0829	0.0216	0.00766	0.0155	2858	0.155, 0.186, 0.233
DD2	2.42	13.20	854	0.1007	0.0272	0.00996	0.0155	3258	0.177, 0.212, 0.265
TMA	2.02	13.85	1192	0.1103	0.0316	0.01229	0.0155	3430	0.186, 0.223, 0.279
TM1	2.21	14.48	1428	0.1059	0.0300	0.01154	0.0155	3644	0.198, 0.237, 0.297

Example 4. J. Read et al., Phys. Rev. D 88, 044042(2013)

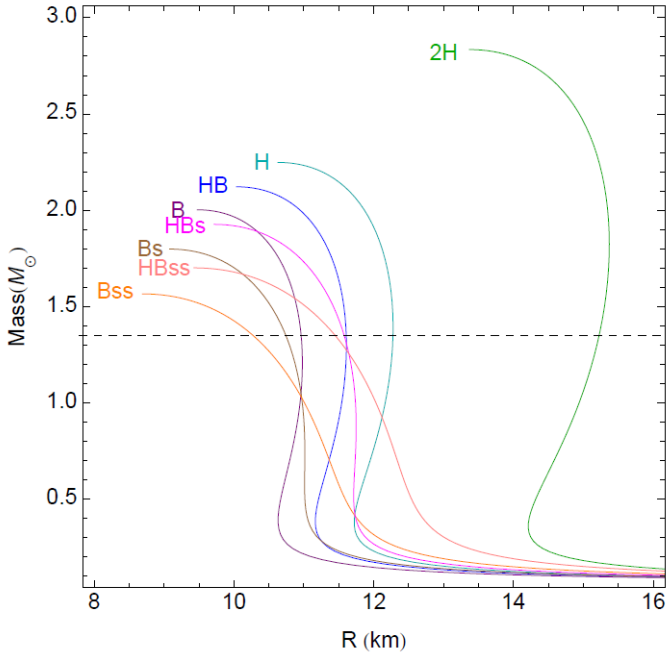

EOS	$\log_{10} p_*$	Γ	R	C	λ	$\Lambda^{1/5}$	Λ
2H	34.9036	3.0	15.23	0.131	10.97	4.713	2325
H	34.5036	3.0	12.28	0.162	2.866	3.603	607.3
HB	34.4036	3.0	11.61	0.172	1.992	3.350	422.0
B	34.3036	3.0	10.96	0.182	1.362	3.105	288.7
Bs	34.3036	2.7	10.74	0.186	1.075	2.961	227.7
Bss	34.3036	2.4	10.27	0.194	0.6695	2.694	141.9
HBs	34.4036	2.7	11.58	0.172	1.770	3.275	376.9
HBss	34.4036	2.4	11.45	0.174	1.421	3.131	301.1

IV. Compact star matter with new scaling law

H. Dong et al., Phys. Rev. C87, 054332(2013);

K. Kim, T. Kuo, HKL, J.Lee M. Rho, arXiv 1412.5380; K.Kim, HKL, J.Lee arXiv1607.03235

W-G. Paneg, T. Kuo, HKL, M. Rho, PRC93,055203(2016)

- Main objective:

1. a consistent way in a unified field theoretic frame work
2. the low and high density regimes are treated on the same footing

- Strategy :

A. Walking ideas
   1. Skyrmions on the lattice → simulation of dense nuclear matter
   2. Hidden local symmetry → vector mesons as gauge bosons
   3. Scale symmetry aspect(trace anomaly) : dilaton

B. Change of scaling law from low density to high density regime

hints from walking ideas

1. topological phase change:
   half skyrmion phase at higher density
2. vector manifestation at high density .
3. two solar mass neutron stars

→ implemented in the scaling with density:
   two different scalings : low - and high density

- nucleon and meson coupling constants
- masses of nucleon and mesons

1. Skyrmion on the lattice: dense nuclear matter

- nucleon as skyrmion (toplogical soliton) in pionic lagrangian

$$\mathcal{L} = \frac{f_\pi^2}{4} Tr(\partial^\mu U \partial_\mu U) + \cdots$$

$$U = e^{i\pi/f_\pi} \qquad \pi = \vec{\tau} \cdot \vec{\pi}$$

$$S^3 \to SU(2) \qquad \boxed{\vec{\pi} \to \vec{r}/r}$$

- baryonic matter : skyrmion on the lattice

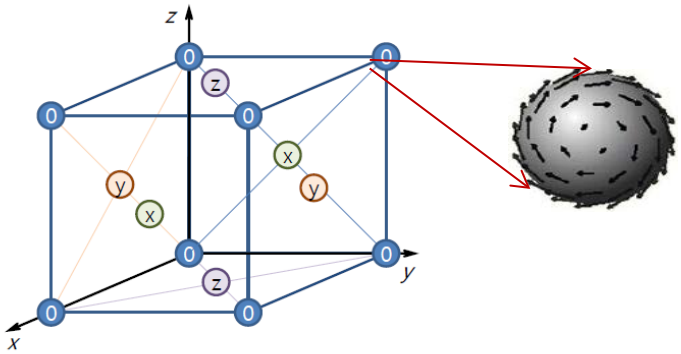

- Half skyrmion phase $n > n_{1/2}$

skyrmions → half skyrmions on lattice

Goldhaber and Manton(1987); Park et al. (2003), …

Skyrmion Crystal

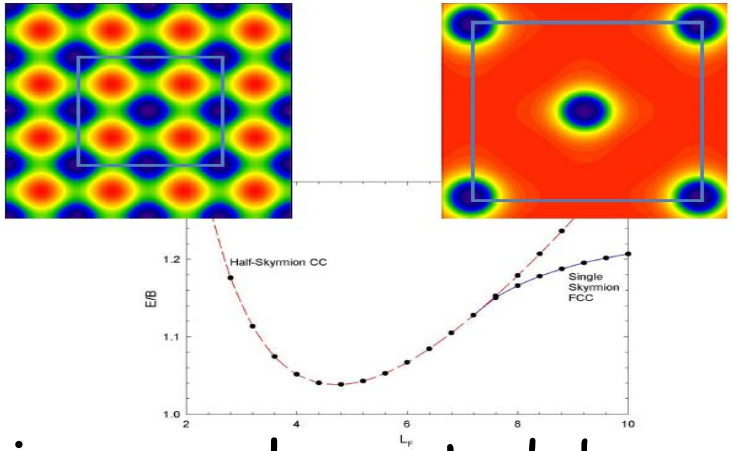

Skyrmion supplemented by a dilaton scalar χ, Park and Vento, 0906.3263

$$\mathcal{L} = \frac{f_\pi^2}{4}\left(\frac{\chi}{f_\chi}\right)^2 \mathrm{Tr}(\partial_\mu U^\dagger \partial^\mu U) + \frac{1}{32e^2}\mathrm{Tr}([U^\dagger\partial_\mu U, U^\dagger \partial_\nu U])^2 + \frac{f_\pi^2 m_\pi^2}{4}\left(\frac{\chi}{f_\chi}\right)^3 \mathrm{Tr}(U + U^\dagger - 2)$$

$$+\frac{1}{2}\partial_\mu\chi\partial^\mu\chi - \frac{1}{4}\frac{m_\chi^2}{f_\chi^2}\left[\chi^4\left(\ln(\chi/f_\chi) - \frac{1}{4}\right) + \frac{1}{4}\right]$$

$n > n_{1/2}$

1. symmetry energy

HKL, Park and Rho, PRC 83,025206(2011)

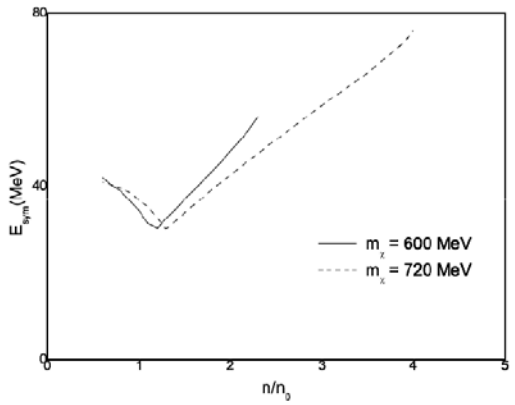

2. homogeneous dilaton condensation $< \chi > \neq 0$

$f_\pi \neq 0$

3. inhomogeneous 'chiral' condensation $\sigma \equiv \frac{1}{2} Tr U, \quad \overline{< \sigma >} = 0$

$(\sim \overline{< \bar{q} q >} = 0)$

Y. Ma et al. Phys. Rev. D 91, 096011 (2015)

2. Hidden local symmetry

$$\mathcal{L}_M = F_\pi^2 \mathrm{tr}\left[\hat{\alpha}_{\perp\mu}\hat{\alpha}_\perp^\mu\right] + F_\sigma^2 \mathrm{tr}\left[\hat{\alpha}_{\parallel\mu}\hat{\alpha}_\parallel^\mu\right] - \frac{1}{2g^2}\mathrm{tr}\left[V_{\mu\nu}V^{\mu\nu}\right]$$

$$\hat{\alpha}_\perp^\mu = \frac{1}{2i}\left[D^\mu\xi_R\cdot\xi_R^\dagger - D^\mu\xi_L\cdot\xi_L^\dagger\right]$$

$$\hat{\alpha}_\parallel^\mu = \frac{1}{2i}\left[D^\mu\xi_R\cdot\xi_R^\dagger + D^\mu\xi_L\cdot\xi_L^\dagger\right]$$

$$D_\mu\xi_L = \partial_\mu\xi_L - iV_\mu\xi_L$$

$$D_\mu\xi_R = \partial_\mu\xi_R - iV_\mu\xi_R$$

$$\mathcal{L}_N = \bar{N}(i\not{D} - m_N)N + g_A\bar{N}\not{\hat{\alpha}}_\perp\gamma_5 N + g_V\bar{N}\not{\hat{\alpha}}_\parallel N$$

- QCD matching and RG

near chiral symmetry restoration : $< \bar{q}q > \to 0$

n ~ n_c

$$m_V \to 0$$

C. Implementation of half skyrmion into nuclear matter: equation of state using $V_{low\text{-}k}$

$0 < n < n_{1/2}$ (Region-I)

old BR scaling at low density

$$\frac{m_M^*}{m_M} = \frac{m_N^*}{m_N} = \Phi_I(n); \Phi_I(n) = \frac{1}{1 + c_I \frac{n}{n_0}}$$

$n_{1/2} < n < n_c$ (Region-II)

new scaling at higher density

$$\frac{m_M^*}{m_M} = \Phi_{II}^M(n); \Phi_{II}^M(n) = \frac{1}{1 + c_{II} \frac{n}{n_0}} \qquad \frac{m_N^*}{m_N} = \Phi_{II}^N(n) = y(n)$$

Region I

$$c_I^N = 0.130, \quad c_I^\rho = 0.121, \quad c_I^\sigma = 0.121 \quad c_I^\omega = 0.139$$

Region II

$$c_{II}^M = c_I^M \qquad c_{II}^N = y(n) \sim 0.8$$

tensor force strength

$$R = \frac{g_\rho m_\rho}{m_N}$$

H. Dong, T. Kuo, HKL, R. Machleidt, M. Rho PRC 87, 054332(2013) , HKL, M. Rho Eur. Phys. J. A50, 14(2014)

Paeng et al. Phys. Rev. C 93, 055203 (2016)

- energy per nucleon

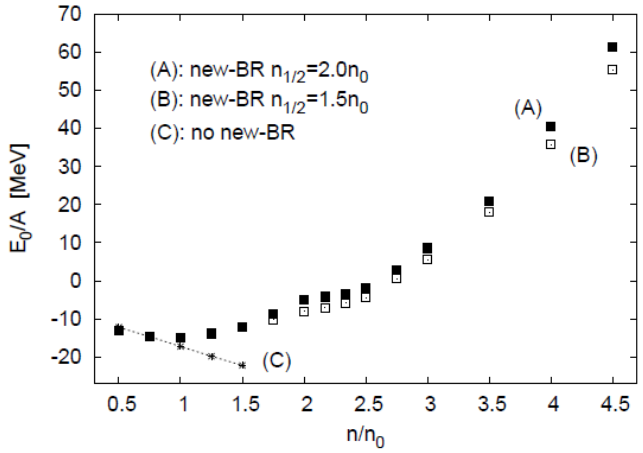

- symmetry energy

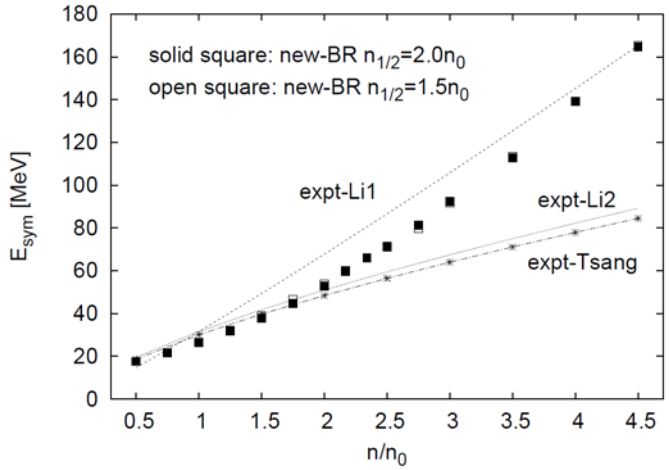

- mass and radius

- central density

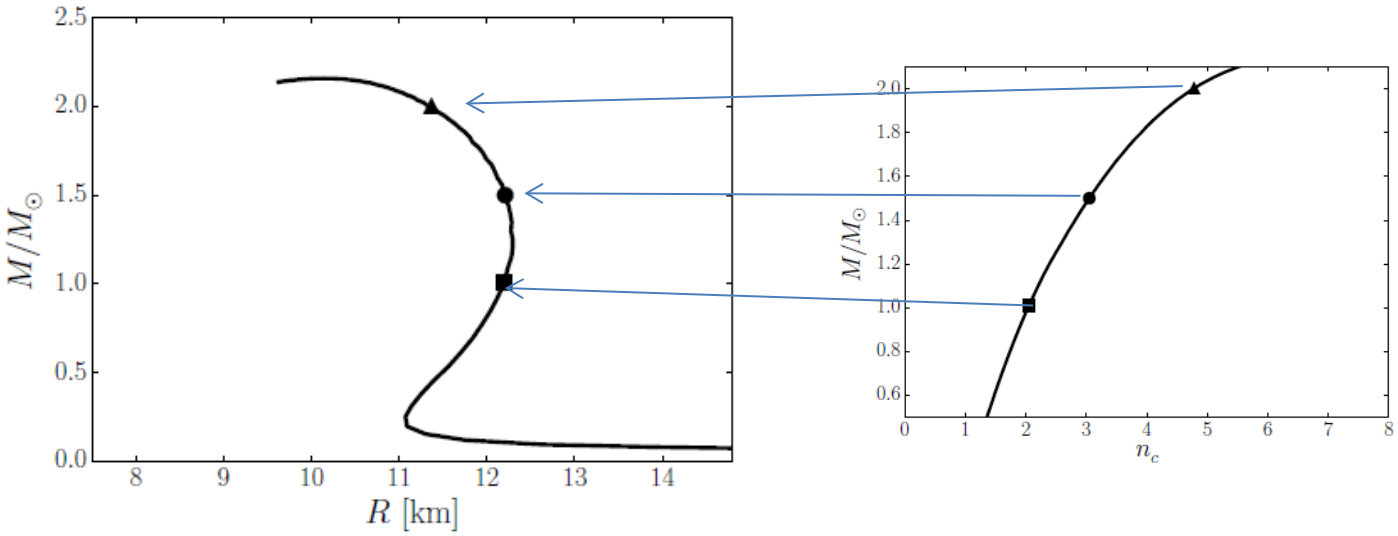

- tidal deformation parameter

K. Kim et al., arXiv:1412.5380; 1607.03235

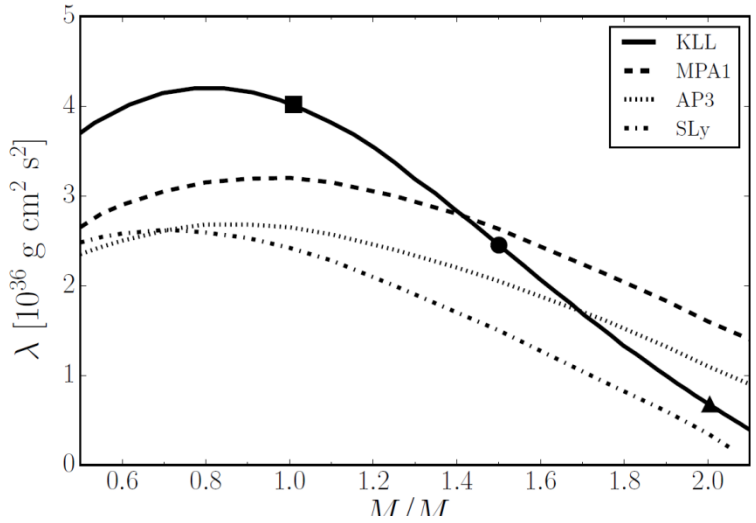

Mass	λ (10^{36} g cm^2 s^2)	Λ
$1.35M_\odot$	3.03	634
$2M_\odot$	0.68	19.6

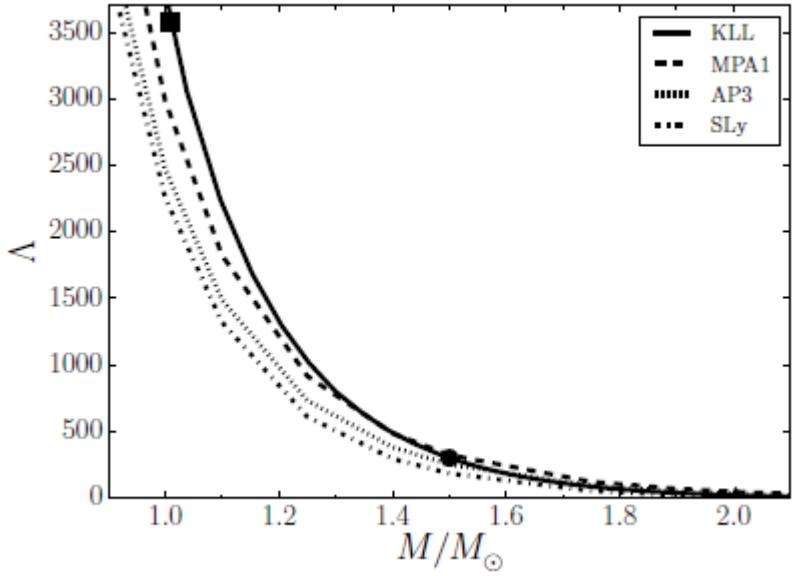

EoS	M_{max} ($M_\odot$)	$R_{1.35}$ (km)	Λ	λ (10^{36} g cm^2 s^2)
APR4	2.20	11.09	322	1.53
SFHo	2.06	11.91	420	2.00
KLL	2.16	12.28	634	3.03
DD2	2.42	13.20	854	4.09
TMA	2.02	13.85	1192	5.71
TM1	2.21	14.48	1428	6.85

V. Observational opportunity for measuring tidal deformation in binary merger

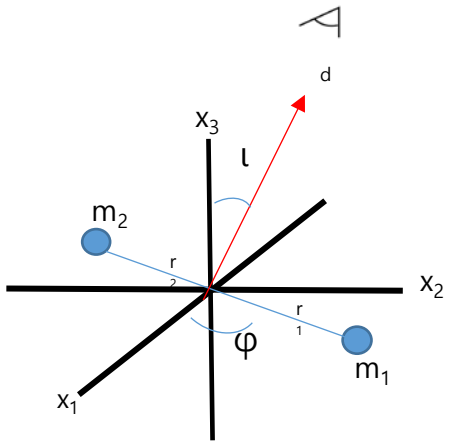

- Gravitational wave: strain amplitude

$$h_+(t) = -\frac{4G\eta M}{c^2 d}\left(\frac{1+\cos^2\iota}{2}\right)x(t)\cos\left[2\Phi(t)\right]$$

$$h_\times(t) = -\frac{4G\eta M}{c^2 d}\cos\iota\, x(t)\sin\left[2\Phi(t)\right]$$

$$x = \left(\frac{GM}{c^3}\frac{d\Phi}{dt}\right)^{2/3} = \left(\frac{\pi G M f}{c^3}\right)^{2/3} \qquad f = 2f_{orbital} = \omega/\pi \qquad \eta = m_1 m_2/M^2$$

- Point particle – stationary emission $\Phi(t) = \omega t$

- Newtonian chirp(inspiral wave form)

$$h_+(t) = -\frac{G\mathcal{M}}{c^2 r}\frac{(1+\cos^2\iota)}{2}\left(\frac{c^3(t_c-t)}{5G\mathcal{M}}\right)^{-1/4}\cos[2\phi_c - \left(\frac{c^3(t_c-t)}{5G\mathcal{M}}\right)^{5/8}]$$

$$h_\times(t) = -\frac{G\mathcal{M}}{c^2 r}\cos\iota\left(\frac{c^3(t_c-t)}{5G\mathcal{M}}\right)^{-1/4}\sin[2\phi_c - \left(\frac{c^3(t_c-t)}{5G\mathcal{M}}\right)^{5/8}]$$

chirp mass $\mathcal{M} = (m_1 m_2)^{3/5}(m_1+m_2)^{-1/5}$

- post Newtonian : point particle and tidal effect

$$\frac{d\Phi(t)}{dt} = \frac{c^3 x^{3/2}}{GM},$$

$$\frac{dx(t)}{dt} = \frac{-\mathcal{L}}{dE/dx}$$

post Newtonian expansion parameter

$$x = v^2 = (\pi M f_{\rm gw})^{2/3}$$

$$E = -\frac{1}{2} c^2 M \eta x \left[1 + e_{\text{PP-PN}}(x;\eta) + e_{\text{Tidal}}(x;\eta,\Lambda_1,\Lambda_2)\right]$$

$$\mathcal{L} = \frac{32}{5}\frac{c^5}{G}\eta^2 x^5 \left[1 + l_{\text{PP-PN}}(x;\eta) + l_{\text{Tidal}}(x;\eta,\Lambda_1,\Lambda_2)\right]$$

post Newtonian : point particle

$$e_{\text{PP-PN}} = \left(-\frac{3}{4} - \frac{1}{12}\eta\right) x + \left(-\frac{27}{8} + \frac{19}{8}\eta - \frac{1}{24}\eta^2\right) x^2 + \left[-\frac{675}{64} + \left(\frac{34445}{576} - \frac{205}{96}\pi^2\right)\eta - \frac{155}{96}\eta^2 - \frac{35}{5184}\eta^3\right] x^3$$

$$\begin{aligned} l_{\text{PP-PN}} = {} & \left(-\frac{1247}{336} - \frac{35}{12}\eta\right) x + 4\pi x^{3/2} \\ & + \left(-\frac{44711}{9072} + \frac{9271}{504}\eta + \frac{65}{18}\eta^2\right) x^2 + \left(-\frac{8191}{672} - \frac{583}{24}\eta\right) \pi x^{5/2} \\ & + \left[\frac{6643739519}{69854400} + \frac{16}{3}\pi^2 - \frac{1712}{105}\gamma - \frac{856}{105}\log(16x) \right. \\ & \left. + \left(-\frac{134543}{7776} + \frac{41}{48}\pi^2\right)\eta - \frac{94403}{3024}\eta^2 - \frac{775}{324}\eta^3\right] x^3 \\ & + \left(-\frac{16285}{504} + \frac{214745}{1728}\eta + \frac{193385}{3024}\eta^2\right) \pi x^{7/2}, \end{aligned}$$

post Newtonian : tidal effect

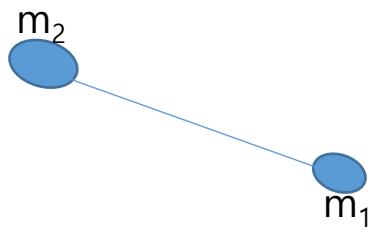

$$\begin{aligned} e_{\text{Tidal}} = {} & -\frac{9\eta}{2}\left[(1-3\eta)(\Lambda_1+\Lambda_2) + \sqrt{1-4\eta}(1-\eta)(\Lambda_1-\Lambda_2)\right] x^5 \\ & - 22\eta\left[\left(1 - 4\eta + \frac{19\eta^2}{8}\right)(\Lambda_1+\Lambda_2) + \sqrt{1-4\eta}\left(1 - 2\eta + \frac{3\eta^2}{8}\right)(\Lambda_1-\Lambda_2)\right] x^6 \end{aligned}$$

$$\begin{aligned} l_{\text{Tidal}} = {} & 3\left[(1-2\eta-4\eta^2)(\Lambda_1+\Lambda_2) + \sqrt{1-4\eta}(1-2\eta^2)(\Lambda_1-\Lambda_2)\right] x^5 \\ & - \frac{22}{7}\left[\left(1 - \frac{15\eta}{176} + \frac{147\eta^2}{88} - \frac{1547\eta^3}{44}\right)(\Lambda_1+\Lambda_2) + \sqrt{1-4\eta}\left(1 + \frac{337\eta}{176} + \frac{15\eta^2}{2} - \frac{1085\eta^3}{88}\right)(\Lambda_1-\Lambda_2)\right] x^6 \end{aligned}$$

- simple exercise

K.Kim et al., preliminary

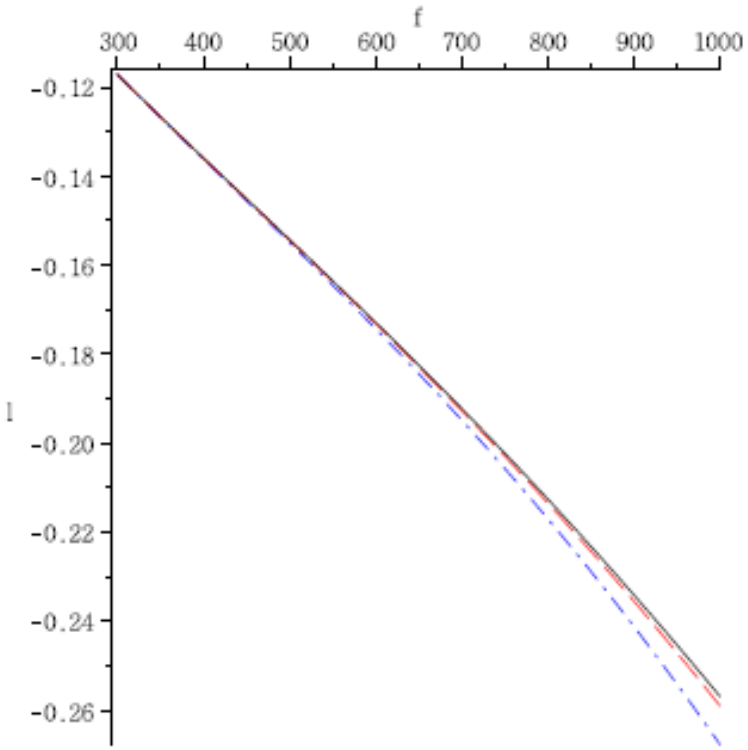

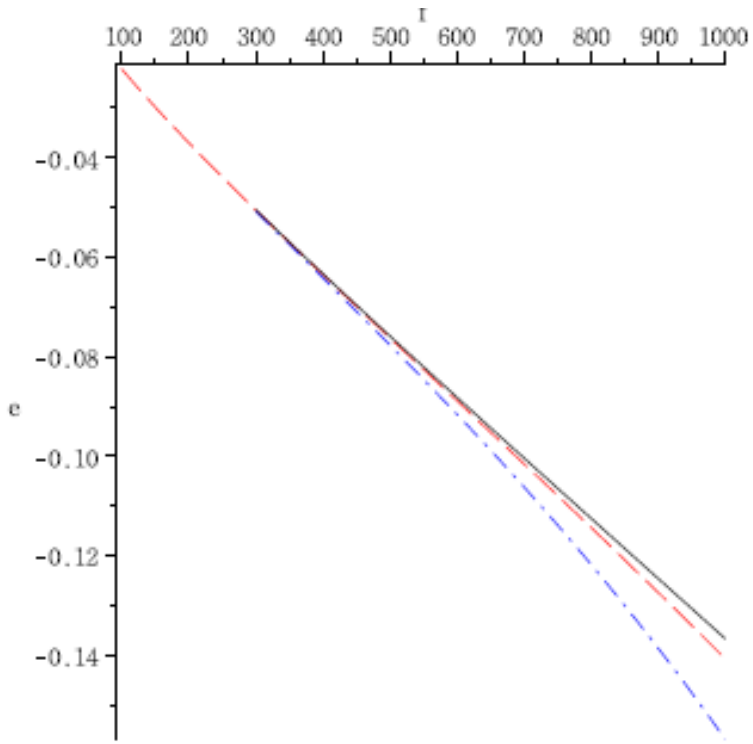

$\Lambda = 0, 200$ and 1000

$M = 2.7 m_\odot$

$l = l_{\text{PP-PN}} + l_{\text{Tidal}}$

$e = e_{\text{PP-PN}} + e_{\text{Tidal}}$

post Newtonian expansion parameter

$$x = v^2 = (\pi M f_{\rm gw})^{2/3}$$

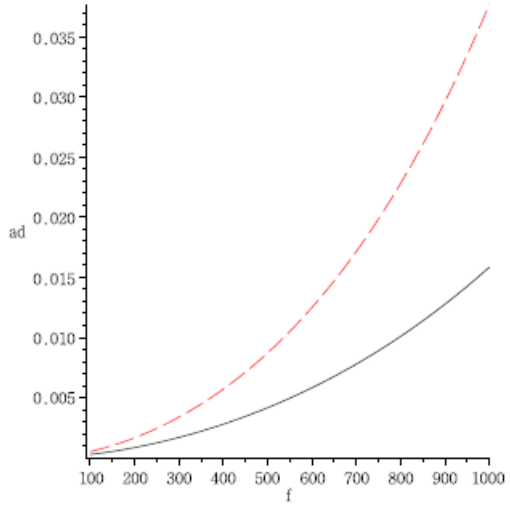

adiabaticity

$$\frac{d\omega/dt}{\omega^2} = \frac{3}{4\pi}\frac{1}{f}\frac{1}{x}\frac{dx}{dt}$$

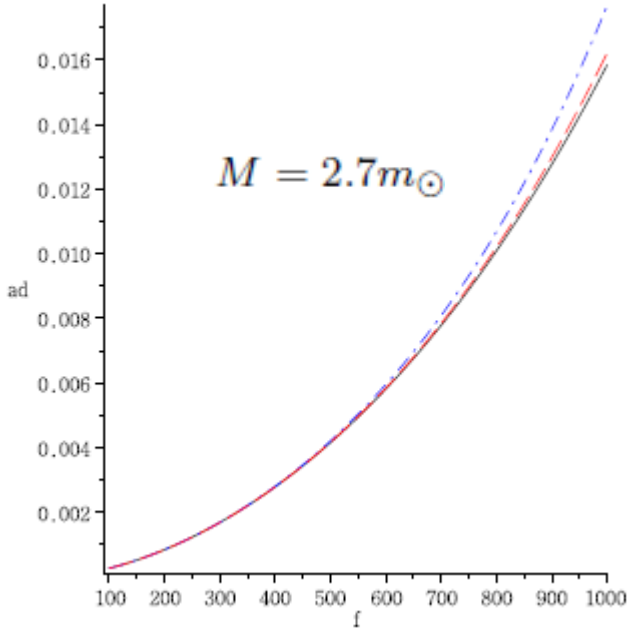

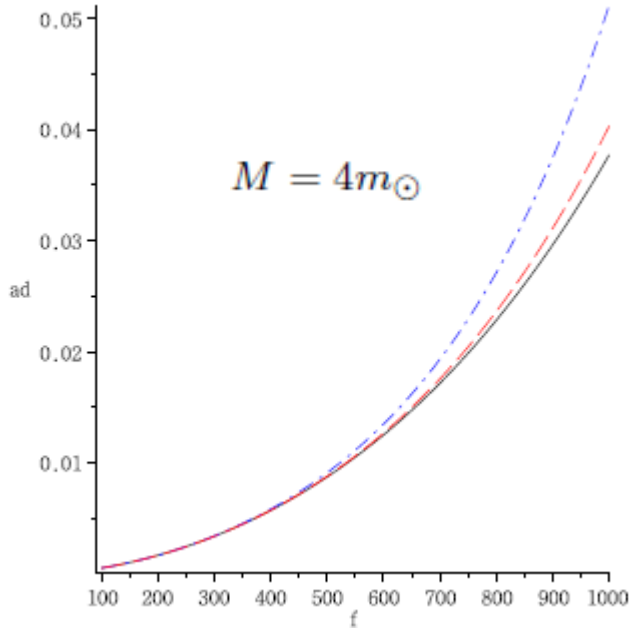

$\Lambda = 0, 200$ and 1000

$1.0m_\odot$ $m = 1.5m_\odot$

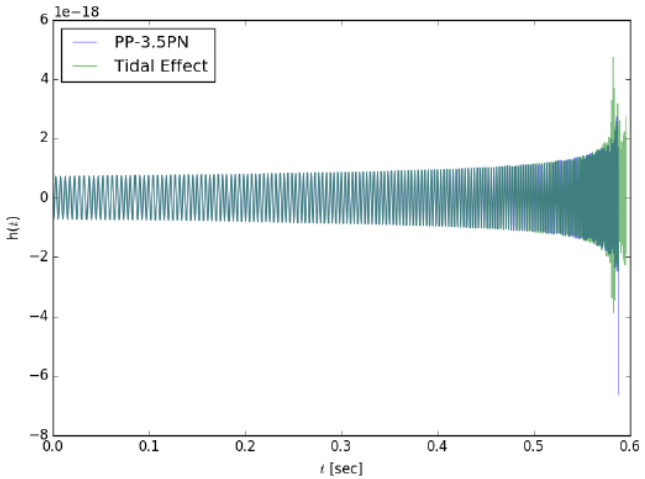

$h(t)$

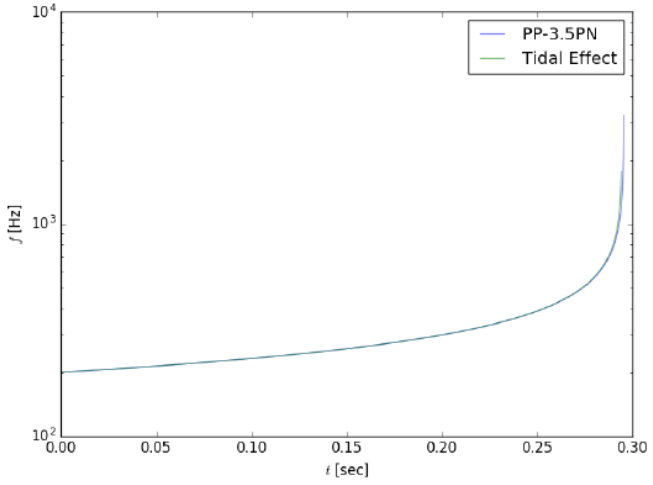

$f(t)$

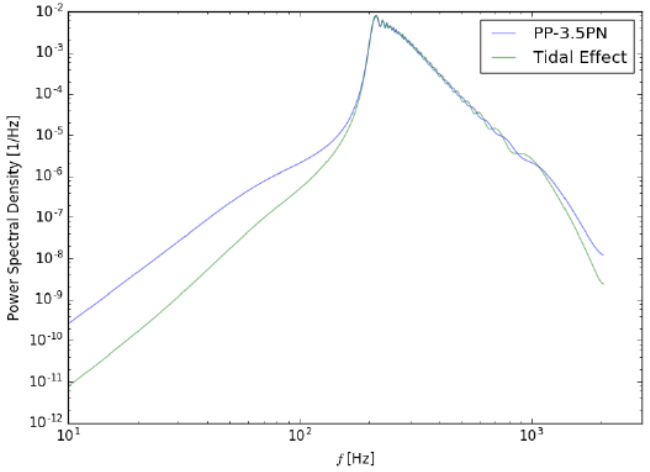

power spectral density

distance: 6.4 kpc (= 1.9748e+20 meter)

- sampling rate: 4096 Hz
- detector's power spectral density for power spectral density of h(t): aLIGO's PSD
- detector's antenna beam pattern response, F_+ and F_x: F_+ = 1 and F_x = 1 (for GWs from z-axis direction)

K.Kim et al., preliminary

• Numerical simulation

- Spectral density curve

Hotokezaka, Kyutoku, Sekiguchi, Shibata. Rev. D93, 064082(2016)

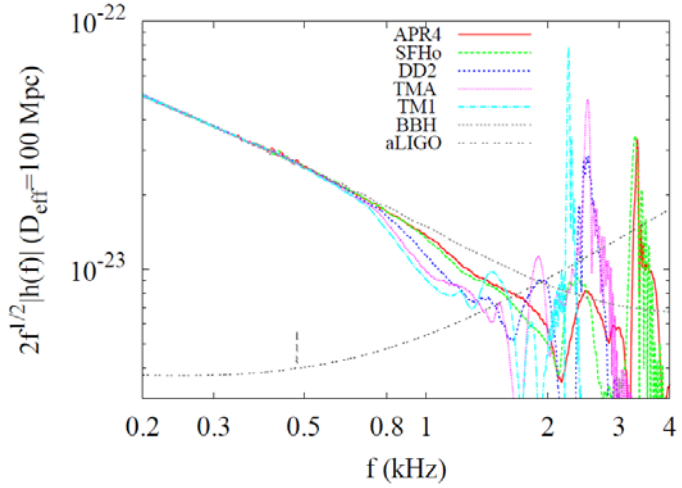

EOS	$M_{\max}$ ($M_\odot$)	$R_{1.35}$ (km)	Λ	$k_{2,1.35}$
APR4	2.20	11.09	322	0.0908
SFHo	2.06	11.91	420	0.0829
DD2	2.42	13.20	854	0.1007
TMA	2.02	13.85	1192	0.1103
TM1	2.21	14.48	1428	0.1059

- distinguishability

$$||h_1 - h_2||^2 := \min_{\Delta t, \Delta\phi} \left[4 \int_{f_i}^{f_f} \frac{\left| \tilde{h}_1(f) - \tilde{h}_2(f) e^{i(2\pi f \Delta t + \Delta\phi)} \right|^2}{S_n(f)} df \right]$$

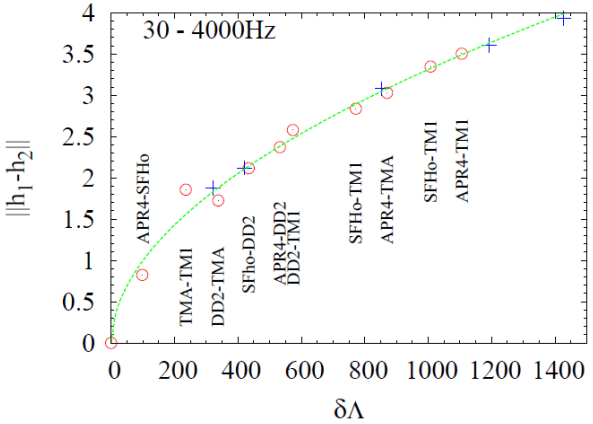

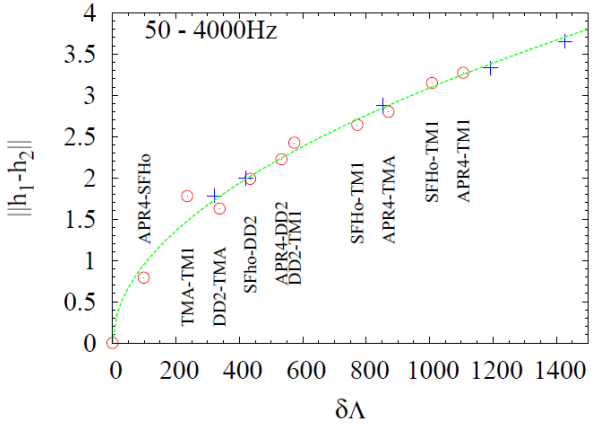

VI. Discussion

- Equation of state of nuclear matter at high density
  - Interactions between nucleon and additional degree of freedoms
- Observables in experiments and observations
  - Particle productions (nucleons, pion and kaons) and their ratio
  - Mass-radius of compact stars
  - Gravitational waves
- Characteristics of EoS relevant to observables
  - Symmetry energy : particle ratio, proton fraction, ….
  - Deformation parameter: gravitational wave
  - EoS up to n ~ 2n_0 – 3 n_0 :
    1. Heavy Ion Machines(FRIB, FAIR, RAON, …) , time scale ~ 10^{-23} s
    2. Neutron star ~ 1.5 solar mass , time scale >> weak interaction
- Ideas on EoS at higher density to be tested
  1. star matter with new scaling law
  2. quarkyonic matter, ……..

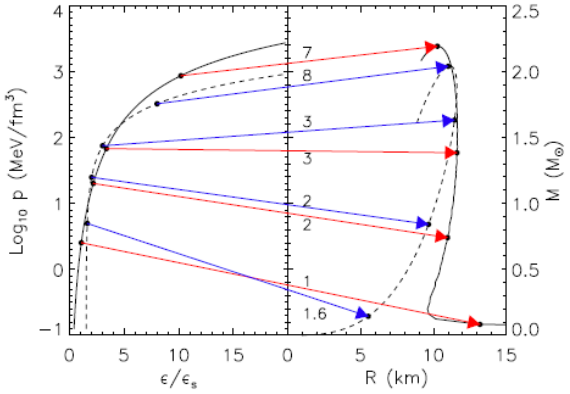

Lattimer, arXiv: 1305.3510

- Characteristic features of equation of state

Symmetry Energy

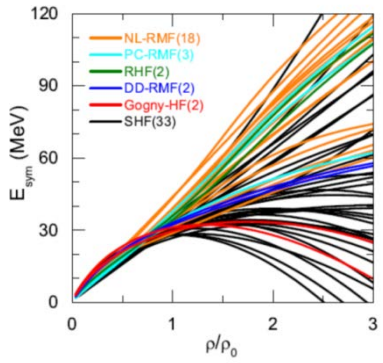

Chen, 1506.09057

Sound velocity

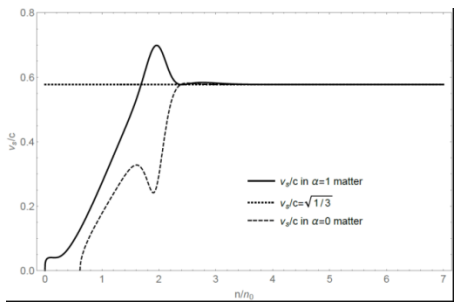

Paeng, & Rho, 1611..09975

Mass -Radius

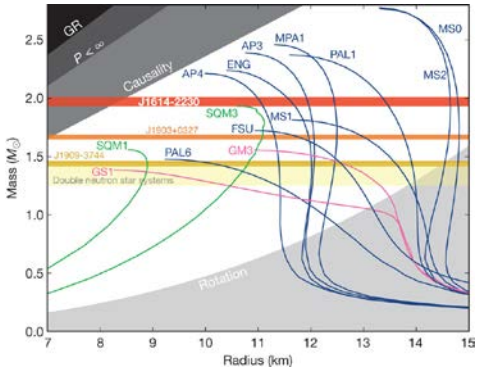

Deformation parameter

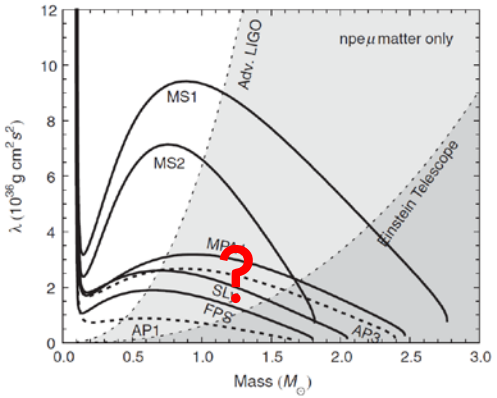

- Observational opportunities in gravitational wave detections at advanced LIGO –Virgo networks(2016 →)

1. Development in analytical and numerical approach
2. Data analysis method to facilitate the details of EoS :
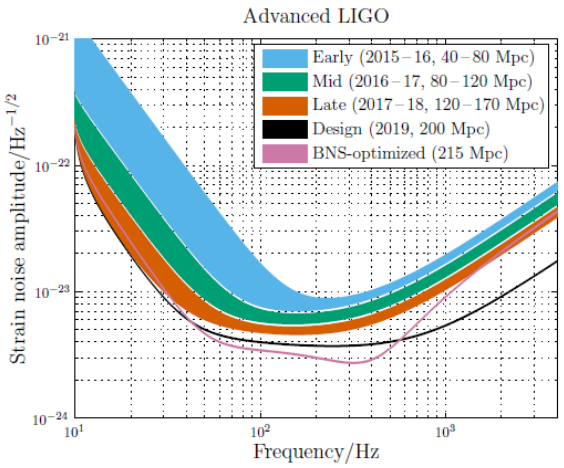
   mass, radius, tidal deformation, …